DESIGN OF PYROLYZER-DESALINATION UNIT INTERFACE FOR DISTRIBUTED BIOCHAR AND CLEAN WATER PRODUCTION

by

Catherine E. Brewer and O. John Idowu

U.S. Department of the Interior
Bureau of Reclamation
Technical Service Center
Water and Environmental Services Division
Water Treatment Engineering Research Team
Denver, Colorado

Month Year

MISSION STATEMENTS

The mission of the Department of the Interior is to protect and provide access to our Nation's natural and cultural heritage and honor our trust responsibilities to Indian tribes and our commitments to island communities.

The mission of the Bureau of Reclamation is to manage, develop, and protect water and related resources in an environmentally and economically sound manner in the interest of the American public.

Disclaimer

The views, analysis, recommendations, and conclusions in this report are those of the authors and do not represent official or unofficial policies or opinions of the United States Government, and the United States takes no position with regard to any findings, conclusions, or recommendations made. As such, mention of trade names or commercial products does not constitute their endorsement by the United States Government.

Acknowledgements

Funding for this research was provided by a Tier 1 Proof of Concept Grant through the New Mexico State University Institute for Energy and the Environment as part of a cooperative agreement with U.S. Bureau of Reclamation.

The authors would like to acknowledge the NMSU Manufacturing Engineering & Technology Center for their assistance with fabricating the lab-scale pyrolyzer, Dr. Kyriacos Zygourakis for his input on the interface design, Mr. Brent Carrillo for his assistance with the pyrolysis runs, Ms. Barbara Hunter for her assistance with soil chemical analyses, Dr. Wayne Van Voohries and Ms. Andrea Salazar for their assistance with HHV analyses, Mr. Graham Hoffman and Mr. Kodanda Phani Raj Dandamudi for their assistance with biochar characterizations, the Idowu research group for their help with the soil incubations, and the staff of the NMSU Department of Chemical & Materials Engineering for their support.

Contents

Page

Glossary

AWC	avaiable water capacity
BF	backward feed
BGNDRF	Brackish Groundwater National Desalination Research Facility
CGT	cotton gin trash
DSG	direct steam generation
EC	electrical conductivity
ED	electrodialysis
FC	field capacity
FF	forward feed
GOR	gain output ratio
HHV	higher heating value
HX	heat exchanger
IEE	Institute for Energy and the Environment
LHV	lower heating value
MED	multiple effect distillation
MSF	multiple stage flash
MSW	municipal solid waste
MVC	mechanical vapor compression
NCG	non-condensable gases
NMSU	New Mexico State University
NOx	nitrogen oxides
PEEK	polyetheretherketone
PF	parallel feed
PHF	polymeric hollow fiber
PP	polypropylene
PP	pecan (orchard) prunings
ppm	parts per million
PS	pecan sheels
psia	pounds per square inch absolute
PWP	permanent wilting point
PV	photovoltaic
RO	reverse osmosis
SAR	sodium adsoption ratio
SOM	soil organic matter
SOx	sulfur oxides
TBT	top brine temperature
TDS	total dissolved solids
TGA	thermogravimetric analysis
TVC	thermal vapor compression
VC	vapor compression
VOCs	volatile organic carbons
YW	yard waste

Executive Summary

Communities located in rural, arid areas face the challenge of finding local and affordable energy supplies to operate water desalination equipment. A renewable distributed energy source that has great potential for water desalination and has yet to be explored is biomass: agricultural wastes, forestry residues, residential yard waste, byproducts from biofuels production, etc. Pyrolysis, a process that transforms biomass through heating under limited-oxygen conditions, can be used to produce char, bio-oil or tar, and non-condensable gas products. The liquid and gas products can be combusted to drive the pyrolysis process, and to provide heat and power to a desalination process. The char product can be applied to soils as biochar to improve soil quality and soil water holding capacity.

The first component of this proof-of-concept project was the theoretical design of a biomass slow pyrolysis system that could be coupled through an interface to a multiple effect distillation (MED) unit for the small-scale desalination of brackish water. The process began with a review of the literature in the overlapping areas of water desalination technologies and renewable energy sources. From the literature review, a low-temperature, parallel feed MED was selected. An ASPEN Plus® chemical engineering process modeling simulation was developed for the interface (furnace, boiler, turbine and heat exchangers) to enable rapid determination of unit operation size and flow stream properties for multiple system size scales and operating conditions. This simulation was used to estimate how much biomass would be needed to produce a given amount of distilled water.

The second component of the project was the production of biochar from locally-available biomass residues and the measurement of those biochars effects on New Mexico soils. Production of the biochars required the design and fabrication of a lab-scale slow pyrolysis reactor system. Pecan shell, pecan orchard prunings, cotton gin trash, and yard waste were used to produce biochars that were amended to and incubated with two agricultural soils. After incubation, multiple soil quality indicators and soil water desorption curves were measured to compare the agricultural potential of amended and unamended soils.

Results indicated that, for an MED producing 1-2 m^3/day of distilled water, approximately 475-550 kg of dry biomass is needed per m^3 of produced distilled water, yielding 160-190 kg of biochar. The pyrolysis-MED concept has potential now as a value-added waste management system; water costs are currently too high (~20-50 US$/$m^3$) for the system to be feasible based on water production alone. Amendment with biochar showed the potential to increase soil organic matter and soil nutrients; biochar salinity is a concern, especially for the cotton gin trash biochar. Biochar appeared to increase the available water capacity of the sandy loam soil although more data is needed to demonstrate statistical significance and evaluate the effect on irrigation management.

Outcomes of this project include four manuscripts to be published as peer-reviewed journal articles, two graduate student theses, four conference presentations, research capacity building in the Water-Energy Nexus for two junior faculty, five follow-on grant proposals, and a process simulation that can be used in future process design.

1. Introduction

1.1 Motivation

Water for agricultural use has become expensive and difficult to obtain in New Mexico and other southwestern states due primarily to an on-going drought. For example, even though they pay approximately $70/acre/year to participate in the Elephant Butte Irrigation District, many NM farmers spend an additional $150-200/acre/year to pump water from their own wells to obtain enough water for cotton or alfalfa crops. This well water can frequently be brackish and its use for irrigation can result in the accumulation of salt in irrigated soils. Soil salinity can result in lower crop yields due to plant salt stress. Treatment of soil salinity often requires flushing the soil with fresh water to transport salts below the root zone. Use of brackish well water to meet temporary water needs can lead to the need for even more fresh water in the long term to maintain crop yield.

Desalination of brackish groundwater is one way to obtain fresh water for irrigation from available water sources. However, desalination requires energy. In rural locations, where many farms are located, electricity from a grid or electricity generation using solid or liquid fuels is often unavailable or prohibitively expensive at the necessary scale. Some desalination systems are designed to use what farmers have available on or near their farms: sunlight, wind, and geothermal energy. Such systems have been employed with some success, although per unit costs remain high. One resource that farmers also have available but that has not been much explored for desalination is biomass in the form of agricultural residues and yard waste. *The primary goal of this project is to explore the feasibility of using biomass to provide the energy needed to desalinate water at the farm scale in rural areas.*

Many agricultural soils in New Mexico are characterized by very low organic matter content and are often poorly positioned to withstand drought and erosion. Thermochemical processing of biomass to produce heat energy for thermal desalination would result in a co-product, biochar, which may help address this soil quality problem. The potential of biochar to increase available soil water is related to its highly porous nature which acts as a sponge and modifies the soil texture. Improvements in soil water use efficiency, and thus, extensions of the time between irrigation events, represent significant potential irrigation water savings. Therefore, *the secondary goal of this project is to measure biochar's ability to improve soil quality and soil water retention properties.*

1.2 Proof-of-Concept Study

1.2.1 Project Objectives

The objectives of this project were to:

- Quantify the resources and conditions needed to enable biomass pyrolysis-powered brackish water desalination.

- Evaluate the potential for biomass pyrolysis-powered brackish water desalination in the context of other desalination technologies.
- Develop the capacity to produce biochars and to conduct biochar-amended soil quality and water use research.
- Evaluate the potential of biochars produced from local biomass resources to improve local agricultural soils.

1.2.2 Project Tasks

The specific tasks undertaken in this project were:

1. Identify scale and configuration of pyrolyzer and desalination unit, including mass and energy balances.
2. Design and prepare fabrication drawings for pyrolyzer-MED unit system components.
3. Construct and perform shakedown trials on lab-scale pyrolyzer.
4. Produce biochars for soil water retention measurements.
5. Prepare and incubate biochar-amended soil samples for soil water retention measurements.
6. Measure soil water potential curves for biochar-amended soils.
7. Prepare final report and proposals for additional external funding.

1.2.3 Project Deliverables

The deliverables of this project are:

a. Selection and sizing of pyrolyzer-desalination unit including mass and energy balances.
b. Design for pyrolyzer-desalination unit system fabrication.
c. Characteristics of slow pyrolysis biochars produced on lab-scale pyrolyzer.
d. Results from biochar-amended soil incubation study.
e. Results and recommendations from biochar-amended soil water potential tests.
f. Final project report.
g. Proposals submitted to external funding agencies.

1.3 Organization of Report

This chapter is intended to provide context for the project and to summarize the take-away messages from the project results.

The second chapter is the text of a review article manuscript prepared by the PhD student on the project during his review of the relevant literature. The manuscript expands on the justification for selection multiple effect distillation (MED) as the desalination technology to be coupled with pyrolysis. The manuscript also provides baseline data of water desalination production rates, water quality and

costs. This text will serve as the literature review chapter of Mr. Ali Amiri's PhD dissertation.

The third chapter presents the results from the pyrolysis-MED interface design process including an Apsen Plus® process simulation and calculations. Assumptions needed for the design led to a reaction and process modeling collaboration with Dr. Kyriacos Zygourakis at Rice University. The results have been presented at two conferences and will be used to prepare an article manuscript and a chapter of Mr. Amiri's PhD dissertation.

The fourth chapter describes the construction and operation of a lab-scale pyrolyzer used to produce biochars from locally available biomass resources. The reactor design, testing, and biochar characterization served as half of the MS thesis work of Mr. Yunhe Zhang, and have contributed to one conference presentation and one article manuscript currently under review.

The fifth chapter presents the methods and results of a soil incubation study using the produced biochars. The soil work is split into two components: general soil fertility and quality, and soil water retention and physical properties. The soil quality results were used in the biochar article currently under review. The soil water retention results are being used to prepare another article manuscript for submission in the near future. The soil water retention work was conducted primarily by two undergraduate researchers, Mr. Brent Carrillo and Ms. Flavia Mitsue Yamashita; continuation and expansion of the work will serve as the MS thesis topic of a new graduate student.

The final chapter summarizes the outcomes from the project.

1.4 Conclusions and Recommendations

Low temperature multiple effect distillation (MED) is the most appropriate water desalination technology to be coupled with biomass pyrolysis due to MED's use of low grade thermal energy, system simplicity, history of coupling with other renewable energy sources at the small scale, and potential for low maintenance operation from the prevention of scaling. Biomass residues contain sufficient energy to provide the heat and power for small-scale water desalination although predicted water costs are still too high for a biomass pyrolysis-MED system to be feasible based on water production alone. Pyrolysis of local agricultural residues produced acceptable yields of biochar with acceptable properties, although the high ash content of the cotton gin trash biochar raises concerns about soil salinity if biochar derived from that feedstock is to be used as a soil amendment.

Further development of biomass pyrolysis-MED systems should be pursued in situations where biomass waste management is the primary objective and where the on-site production of small amounts of high-purity water is needed; soil quality and soil water effects of applied biochars may provide additional value to the system and should be investigated. Design of biomass pyrolysis-MED

prototypes should be based on scale and suitability of unit operations (especially steam turbine generators), followed by the availability (amount, seasonality, cost) of biomass in the near vicinity. More research is needed on the relationship between biochar ash content and its effect on soil salinity and crop yields. In some cases, the effects of increased salinity might be offset by changes in other soil quality indicators; if biochar salinity is limiting, methods for quantifying that limitation are needed. More research is needed to understand the impacts of biochar amendments on soil's available water capacity, especially for irrigated cropping systems. Research efforts should strive to align instrumental/theoretical measurements with crop-relevant impacts in the field.

2. Energy Sources for Water Desalination Literature Review

Abstract

Water desalination is an energy-intensive process needed in many parts of the world to provide fresh water for drinking, agriculture, and industry. The energy for desalination can come from conventional fossil fuels such as petroleum, natural gas and coal, as well as renewable energy sources such as solar, wind, hydro, and geothermal. One renewable energy source that is widely available but currently unused for water desalination is biomass. In this review, we summarize available water desalination technologies, energy requirements and costs, and explore how scale and resource availability create trade-offs in technology selection and design. From there, we present a case for the circumstances in which biomass energy may be suitable for water desalination: small scale capacity needs, infrastructure-poor or rural areas, lower-salinity (brackish) source water, thermal desalination technologies, and an abundant, underutilized biomass supply.

2.1 Introduction

The need for high quality water is dramatically increasing due to rapid population growth, higher per capita water consumption, greater industrial and power generation water use, and expanding agricultural production. Freshwater resources are not capable of meeting these needs as just 3% of earth's water is fresh water. As such, there is need for techniques to purify available but low-quality water. Water desalination is a common technique for providing large quantities of high quality, potable water worldwide. Approximately 50% of the desalination plants are located in the Middle East, 20% in the US, 18% in Europe, and 12% in Asia (Raluy, et al., 2005). The installed desalination capacity throughout the world in 2000 was about 22 million m^3 of water per day, requiring approximately 8.5 EJ of energy per year, which is equivalent to 203 million tons of crude oil. Concerns about petroleum-based energy availability and environmental impacts have motivated the exploration of alternative and renewable energy sources for water desalination (Kalogirou, 2005).

In this review, we summarize desalination technologies and energy sources, focusing on multiple effect distillation (MED) and renewable energy. From this summary, we present an argument for the potential of biomass as an energy source for water desalination through a pyrolysis-MED process.

2.2 Desalination

2.2.1 Water Quality and Technologies

Water quality is categorized as a function of total dissolved solids (TDS) in parts per million (mg/L): freshwater contains 200 to 700 ppm, treated wastewater contains 700 to 1,500 ppm, brackish water contains 2,000 to 10,000 ppm, and

seawater contains 30,000 to 60,000 ppm. Approximately 58% and 23% of the installed water desalination capacity worldwide are used for treating seawater and brackish water, respectively (Eltawil, et al., 2009). In addition to dissolved salts, waters can contain other impurities such as microorganisms, organic matter, suspended solids, silica, etc. that can cause scaling, fouling, and corrosion in the unit. For this reason, efficient pre-treatment and post-treatment techniques to eliminate harmful impurities are often needed.

Depending on the TDS of the water, treatment costs, and infrastructure availability, a variety of desalination techniques can be used; these techniques are grouped into membrane/single-phase processes and thermal/phase-change processes. There are also some new approaches for desalination. Some examples are forward osmosis, ion concentration polarization, super-cavitation evaporation, and capacitive deionization (Kalogirou, 2005, Likhachev and Li, 2013, Raluy, et al., 2005, Semiat and Hasson, 2012).

2.2.2 Membrane Processes

The two main membrane desalination processes are electro dialysis (ED) and reverse osmosis (RO). Both require electrical energy to drive the separation process. In ED, anion-permeable and cation-permeable membranes, in combination with a cathode and an anode, are used to draw salt ions outward from a dilute feed steam into concentrated brine streams. The electrical power is used to maintain a voltage across the anode and cathode. ED systems, which were developed almost 10 years before RO, are usually used to treat brackish water, and they are more efficient for higher concentrations of highly mobile, small ions.

In RO, which is responsible for more than 88% of the membrane process capacity worldwide, hydraulic pressure is used to overcome osmotic pressure to force water molecules through a semi-permeable membrane (pore sizes less than 10 Å) from a stream with low ion concentration to a stream with high ion concentration. The osmotic pressure, π, is dependent on the TDS of the dilute and concentrated streams:

$$\pi = \frac{\varphi \gamma c R T}{M}$$

where γ is the number of ions, φ is the osmotic coefficient, c is the difference in salt concentration between the two streams on a mass basis, M is the salt's molecular weight, R is the gas constant, and T is the temperature in Kelvin (Semiat and Hasson, 2012). For RO to work effectively, the hydraulic pressure provided by a pump on the dilute stream side of the membrane must be significantly higher than the osmotic pressure. RO is usually more cost-effective for water with TDS values less than 5,000 ppm, while ED is more economical for water with TDS values greater than 5,000 ppm (Al-Karaghouli and Kazmerski, 2013, Eltawil, et al., 2009).

For both ED and RO, membrane scaling and fouling can substantially affect system performance. Water pre-treatments such as filtration, sterilization, and/or

chemical additives can be used to prevent scaling and bio-fouling (Al-Karaghouli and Kazmerski, 2013, Braun, et al., 2010). Compared to thermal desalination systems, membrane processes usually have less risk of scaling and corrosion due to membrane processes' ambient or near-ambient operating temperatures (Eltawil, et al., 2009). Post-treatment processes for membrane desalination systems can include hydrogen sulfide removal and/or pH adjustment, depending on the final intended water use. More detailed information on membrane desalination process design and membrane scaling can be obtained in (Braun, et al., 2010, Elimelech and Phillip, 2011).

2.2.3 Thermal Processes

There are three main types of thermal desalination processes: multi-stage flash distillation (MSF), vapor compression distillation (VC), and multiple effect distillation (MED). All three require low-temperature heat as the main energy input and a small amount of electricity to drive pumps. Some advantages of thermal desalination processes over membrane desalination processes are higher quality product water, no membrane replacement costs, lower sensitivity to changes in feed water quality, and less rigid monitoring requirements (Eltawil, et al., 2009, Hanson, et al., 2004, Kalogirou, 1997).

2.2.3.1 Multi-Stage Flash Distillation (MSF)

MSF was first developed by Silver at Weir Co. in Glasgow, Scotland in 1960 and is based on seawater evaporation using steam from an external heat source. For many years, MSF has been the "easiest" technology for water desalination and accounts for over 40% of desalination technologies worldwide (Al-Karaghouli and Kazmerski, 2013, Likhachev and Li, 2013). The typical capacity for an MSF process is large: 10,000 to 35,000 m^3/day. In MSF, seawater is preheated using heat exchangers up to 90-110˚C before entering the first stage. Vacuum pumps create a negative pressure difference near seawater's saturation point in the first stage, causing the seawater to partially flash. The flashed water vapor is condensed by contact with the incoming seawater in the heat exchangers and collected. The remaining concentrated seawater/brine enters the second stage, which is operated at a lower pressure than the first stage. Again, the negative pressure difference causes some of the seawater to flash off and be collected. This process continues until the last stage, which has the lowest temperature and pressure. Sometimes, demisters are used to remove entrained brine droplets from the flashed vapor as these droplets can create salinity in the product water and contribute to scale formation on condenser tubes. The vacuum system removes produced non-condensable gases in order to keep the heat transfer coefficient as high as possible within the stages. To prevent scaling, pre-treatments such as adding acid or advanced scale inhibitors like polyphosphate can be used.

2.2.3.2 Vapor Compression (VC)

VC is very similar to MSF but only has one evaporation stage and can be run under atmospheric or sub-atmospheric pressure. Hot, pressurized feed water

enters the evaporation stage and flashes off, then is condensed and collected. The remaining brine can then be recycled through the process by re-pressurizing it. The VC pressurization can be done using mechanical vapor compression (MVC), which requires additional electricity energy for the pump, or thermal vapor compression (TVC), in which high-pressure steam is injected into the feed stream (Al-Karaghouli and Kazmerski, 2013, Semiat and Hasson, 2012).

2.2.3.3 Multiple-Effect Distillation (MED)

MED, also known as multiple-effect boiling (Kalogirou, 2005), is the oldest thermal desalination process and has a typical plant capacity of 600 to 300,000 m^3/day. MED has been in competition with MSF technically and economically for many years. At the end of 2011, MSF and MED units accounted for approximately 26% and 8.2% of worldwide water production capacity, respectively (2012). Two main advantages of MED over MSF are MED's lower energy consumption due to better heat transfer from the constant temperature difference in MED effects, and the fewer number of effects needed in MED to achieve a given performance ratio (mass of distillate produced per unit mass of input steam) (Al-Karaghouli and Kazmerski, 2013, Kalogirou, 2005).

In the most common configuration of MED, steam from an external heat source is fed into a tube in the first effect. Seawater or brackish water is sprayed onto the steam-filled tube and part of the water flashes into steam. The newly produced steam is then fed into the next effect as the heat source, after which it condenses and is collected. As in MSF, temperature and pressure decrease from the first effect to the last effect (Al-Shammiri and Safar, 1999, Semiat and Hasson, 2012, Sen, et al., 2011).

An important design parameter for MED is the gain output ratio (GOR): the ratio of distilled water to input steam flow rates. GOR represents the number of times that the heat of evaporation is reused (Al-Karaghouli and Kazmerski, 2013, Joo and Kwak, 2013, Likhachev and Li, 2013, Manenti, et al., 2013, Semiat, 2008); GOR relates directly to energy efficiency. Yang et al. showed that GOR and water production rate decrease with increasing feed water flow rate and increase with increasing steam flow rate (Yang, et al., 2011). Zhao et al. observed that, although increasing the feed steam temperature slightly decreased GOR, such a temperature increase decreased the total heat transfer area needed—a result of a greater temperature difference between adjacent evaporators (Zhao, et al., 2011).

Another important factor in MED design is the optimization of the number of effects. This number is a function of the temperature difference between the feed steam and the top brine temperature (TBT), as well as the minimum temperature differential within an each evaporator (Ophir and Lokiec, 2005). Having more effects results in more distilled water produced and a higher GOR, however, the capital cost and per kg distilled water cost also increase. Other design factors include TBT and heat transfer area within the effects. At higher TBTs, the number of the effects increases and thus the GOR increases. Generally, an MED can be

operated at either a high TBT (> 90°C) or a low TBT (55-90°C). Although the heat transfer area and the water production costs for high TBTs are much less than those for low TBTs, high TBTs dramatically increase the amount of corrosion and scaling, as well as the energy consumption. For this reason, low TBT MED is more widely used worldwide than high TBT MED (Miller, 2003, Ophir and Gendel, 2006, Zhao, et al., 2011).

2.2.4 MED Design Considerations

2.2.4.1 Feed Arrangements

There are three main flow arrangements in MED unit design: forward feed, backward feed, and parallel feed; each arrangement has its own advantages and disadvantages. In the forward feed (FF) arrangement, which is the most common configuration, feed water and steam move in a same direction. As shown in Figure 2.1.a, the feed water and steam both enter the system in the first effect at their highest temperature and pressure. One of the challenges for the FF arrangement is that a large portion of the energy is required in first evaporator to heat the feed water to its boiling point, meaning that the heat transfer surface area in the first effect is much greater than in the other effects. Regenerative heat exchanges between effects can solve this problem: steam exiting one effect transfers a small amount of its energy to pre-heat the feed stream before moving on to the next effect. Figure 2.1.b shows how such heat exchangers can be used to heat feed water from an initial feed water temperature to a temperature much closer to the boiling point before entering the first effect.

In the backward feed (BF) arrangement, the feed water enters the last effect where the temperature and pressure are lowest. The steam enters the system in the first effect, where it comes in contact with the highest salinity brine. The advantage of this system is that high-salinity brine evaporation, which requires the most energy, is done at the highest temperature. The disadvantages of this arrangement are that the high temperatures, pressures, and salinities in the first effect can cause more scaling and fouling, and the movement of feed water from low pressure to high pressure requires additional pumping between effects. Part of the increase in scaling and fouling is because the solubility of calcium salts decreases at higher temperatures.

In the parallel feed (PF) arrangement, new feed water is injected at the top and brine is collected from the bottom of each effect independently, while the heat transfer fluid (feed steam and produced water vapor) still move from one effect to another. In such an arrangement, the salinity within each effect reaches its maximum value, meaning that the greatest amount of fresh water vapor had been removed. Darwish et al. showed that the PF arrangement has larger GORs than FF or BF for 2-6 effects, with the difference in GOR increasing with the number of effects (Darwish and Abdulrahim, 2008).

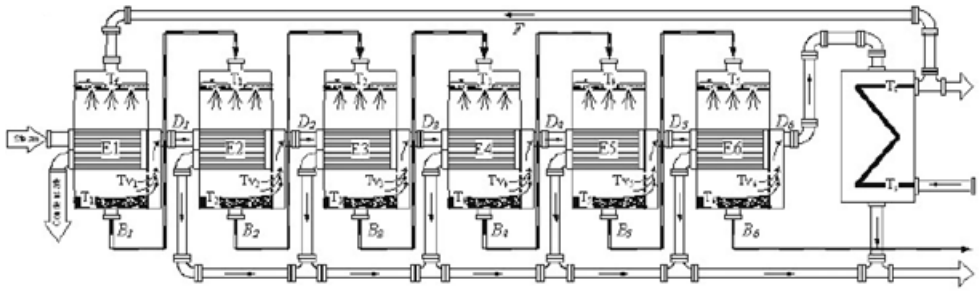

(a)

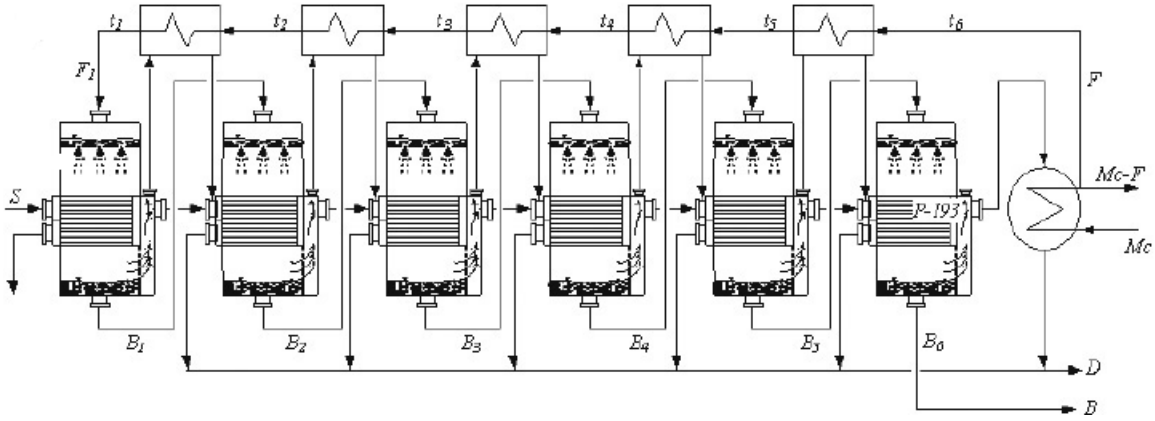

(b)

Figure 2.1. (a) Forward feed flow arrangement and (b) forward feed flow arrangement with regenerative heat exchangers in a six effect, horizontal tube water spray MED unit (Darwish and Abdulrahim, 2008).

In addition to the direction of the flow, the side of the heat exchanger (tube side or shell side) in which each steam flows also impacts MED design. Flowing the steam on the tube side and feed water on the shell side has some advantages: less mist carry-over in the produced steam, easier scale removal/cleaning, and easier turbulence generation inside the tubes, which improves heat transfer (Sen, et al., 2011).

2.2.4.2 Scaling and Fouling in MED

Scaling decreases the overall heat transfer coefficient in heat exchangers because of the low thermal conductivity of the scale material. In MED heat exchangers, scale build-up on the outer surface of evaporating tubes increases the wall temperature of the tubes, which, over a prolonged period of time, can lead to crack formation in the tubes, in addition to lower overall MED energy efficiency (Al-Anezi and Hilal, 2007, Al-Jaroudi, et al., 2010).

Scale formation within MED units is dependent on the concentrations of Ca^{2+}, Mg^{2+}, bicarbonate, and TDS in the water; operating temperature; water residence time; fluid velocity; water pH; rate of CO_2 release; and the roughness of the evaporator construction materials (Al-Anezi and Hilal, 2007, Al-Jaroudi, et al., 2010). There are different types of scale deposits including soft, hard, silica, and organic. In research with a MED-VC unit, Al-Jaroudi, et al. observed a 14 mm-

thick scale build-up comprised of soft $CaCO_3$ and hard $CaSO_4$, as well as a significant proportion of organic matter (Al-Jaroudi, et al., 2010). There are three ways to control build-up of $CaSO_4$ scale: decrease the MED operating temperature, decrease the overall concentration factor (brine TDS/feed water TDS) to keep the brine TDS concentration below the scaling threshold, and soften the feed water by substituting a monovalent cation such as Na^+ for the Ca^{2+}. Magnesium hydroxide is an alkaline scale component that is sometimes observed in MSF or MED systems from high Mg^{2+} ion concentrations in the water. Polyphosphate may be used as a scale inhibitor if the unit's operation temperature is less than 90°C; hydrolysis of polyphosphate occurs at higher temperatures, which leads to the formation of calcium phosphate. For this reason, polyphosphate is rarely used for MED units. The presence of organic matter in scale build-up may be due to marine life (bio-fouling) or from industrial discharges of oil, grease, wax or paint materials. A hot alkaline treatment can usually remove organic scale build-up. Similar to scale prevention in MSF, water pre-treatments, a vacuum system, and a demister can also be used to avoid scaling in MED. Even with several management techniques, there is still a chance of scaling in MED units (Al-Jaroudi, et al., 2010).

2.2.4.3 Scaling and Non-Condensable Gases

Non-condensable gases such as CO_2, O_2, and N_2 are released during brine evaporation within the effects or through ambient air leakage into the parts of the unit operating under vacuum. The presence of these gases may cause alkaline scale formation. For example, the combination of dissolved CO_2 in the condensate, which decreases the water pH to acidic conditions, with O_2, may cause corrosion in condenser tubes. De-aeration of the feed water in a titanium tube condenser is a method to decrease the oxygen content within the feed water. CO_2, which dissociates in water to form $HCO_3^-$and CO_3^{2-}, is harder to manage. The release rate of CO_2 is highest in the first effect, and at higher water temperatures and salinities (Al-Anezi and Hilal, 2007, Ophir and Gendel, 2006). $CaCO_3$ scale deposition is also highest in the first effect and pH decreases from the first effect to the last effect (Al-Rawajfeh, 2010). Even a low concentration of non-condensable gases within the water can significantly decrease the overall heat transfer coefficient over time, leading to a decrease in evaporator performance (Al-Anezi and Hilal, 2007). For these reasons, an efficient venting system is critical to control the release of non-condensable gases and prevent scaling, fouling, poor heat transfer, and ultimately, increased energy consumption (Al-Rawajfeh, et al., 2004).

2.2.4.4 Scaling and Tube Construction in MED

There are many different ways of arranging the water flow patterns and the steam tubes within MED heat exchangers: water tube-side vs. steam tube-side, falling water film vs. water spray vs. water immersion, horizontal tubes vs. vertical tubes, smooth tubes vs. corrugated tubes, etc. Four common evaporator combinations are: vertical steam tube-side, vertical water tube-side, horizontal steam tube-side (see Figure 2.1), and horizontal water tube-side. Among them, horizontal steam

tube-side with a falling film water flow has been found to be the most efficient arrangement in terms of energy consumption, thermal characteristics, and simplicity in construction. A tube falling film arrangement is preferred in industry because it lowers the frequency of scaling and carry-over in the tubes due to shorter contact time between the brine and the heat transfer surface, and lowers the vapor velocity which increases the overall heat transfer coefficient, leading to a higher MED system efficiency (Likhachev and Li, 2013, Ophir and Lokiec, 2005). Galal et al. showed that the amount of water that can be condensed on the outer surface of corrugated tubes is 1.5 times greater than the amount that can be condensed on smooth tubes. Also, the fouling thermal resistance of corrugated tubes is nearly half that of smooth tubes, leading to higher long-term thermal performance (Galal, et al., 2010).

For low TBT MED, aluminum is preferred over copper because more aluminum tubes can be installed for the same investment costs, leading to more heat transfer area and higher thermal efficiency per amount of produced water; for high TBT MED, however, copper is preferred (Ophir and Lokiec, 2005). Zarkadas et al. studied polymeric hollow fiber (PHF) heat exchangers made of polypropylene (PP) and polyetheretherketone (PEEK), and found that they have the same or even better thermal performance than metal heat exchangers (Zarkadas, et al., 2005). Other advantages of PHF heat exchangers over metallic ones include smaller volumes, significantly lower pressure drops, less weight, and better resistance to corrosion. The disadvantage of most PHF heat exchangers is that they have a low thermal conductivity (0.1-0.5 W/m·K); this disadvantage can be minimized by using a very small wall thickness (Yan, et al., 2014). Christmann et al. [34] tested a pilot-scale MED with falling film plate evaporators composed of PEEK with wall thicknesses of 25 μm and found that the thermal conduction resistance was 10^{-4} K/W, which is the same as that of stainless steel with a wall thickness of 1.5 mm (Christmann, et al., 2010). The low mechanical strength of polymers, however, means that some stabilization measures must be taken if the walls are to withstand pressure differences across the heat transfer surface (Christmann, et al., 2010, Hetsroni and Mosyak, 1994, Zaheed and Jachuck, 2004).

2.2.5 Hybrid Desalination Systems

In hybrid desalination systems, a power generation unit is combined with both thermal and membrane processes; such systems are more efficient and economical than “dual-purpose” evaporation systems, where the power generation unit provides both electrical and thermal energy required for desalination but only one kind of process is used (Ophir and Lokiec, 2005, Uche, et al., 2001). For instance, in RO-MSF, the water exiting the RO unit is fed into an MSF unit. This increases the overall amount of very pure distilled water (since MSF can achieve a lower exit TDS concentration than RO) and decreases the cost of a pre-treatment unit (since the RO system removes most of the salts that would cause scaling problems in the MSF system). An MED-RO or MSF-RO system is also viable, where pre-heated seawater exiting the last effect of an MED or MSF distiller is fed into an RO unit. In this case, a 1°C increase in seawater feed temperature boosts the water

production rate in RO by 3% (Hamed, 2005). More information on hybrid systems is available in (Cardona, et al., 2003, Hamed, 2005, Helal, et al., 2003, Helal, et al., 2004, Manolakos, et al., 2001, Thu, et al., 2013).

2.3 Biomass as an Energy Source

Biomass is unique among renewable energy options in that it can be both a source of energy and a source of materials. In this way, biomass is similar to petroleum and coal. According to the US Department of Energy's 2011 report, the total annual energy consumption in the US is approximately 98 billion GJ, 4% of which comes from biomass. The annual biomass production rate in the US is approximately 214 million Mg: 129 million Mg as forest resources and 85 million Mg as agricultural resources (Brown and Brown, 2014, Quaak, et al., 1999). Compared to energy from petroleum or coal, energy from biomass has several disadvantages: 1) lower bulk densities, 2) lower energy contents, 3) higher moisture content (which can create both transportation and storage problems due to weight and decomposition, respectively), and 4) greater heterogeneity (Zanzi, 2001). More information about the challenges and prospects of first and second generation biofuel production from biomass is available in (Yousuf, 2012) and (Naik, et al., 2010).

2.3.1 Biomass Types and Sources

Biomass used for energy usually comes from one of two categories: wastes or dedicated energy crops. Wastes include yard waste, municipal solid waste (MSW), agricultural residues (e.g. rice husks, grain straw, orchard prunings), food waste, logging residues, and animal manure. The main advantage of waste biomass is its relatively low cost; its main disadvantage is the large variation in availability, composition, and characteristics from one season to another, and one location to another (Garcia-Perez, et al., 2012).

Dedicated energy crops are plants specifically grown for energy production. They include herbaceous crops such as switchgrass and miscanthus, short rotation woody crops such as hybrid poplar, and oleaginous (lipid-rich) crops such as oilseeds and yeasts. Energy crops are optimized for high rates of biomass production and/or high yields of specific plant components, such as fatty acids in oleaginous crops. While food crops (i.e. plant components that contain significant amounts of digestible carbohydrates, proteins, and/or fats) can be used for energy, a goal of dedicated energy crops is to not compete with food production or use prime land resources. Among woody crops, hardwoods such as willow, polar, mesquite, and alder, are preferred for most conversion techniques over softwoods due to their lower lignin content. Softwoods, such as pine, are beneficial for construction and thus make up a significant portion of logging and construction residues; these residues are typically used as boiler fuels (Brown and Brown, 2014). In spite of their overall lower productivities compared to herbaceous or woody energy crops, oleaginous crops are popular because they contain long-chain hydrocarbons and relatively low amounts of oxygen, and thus resemble

petroleum. For example, soybean and sunflower only produce about 450-1,600 L of biodiesel per hectare compared to corn which can produce 5,800-8,700 L of ethanol per hectare. The hydrocarbons in oleaginous crops include sterols, fatty acids, di-glycerides, tri-glycerides, and waxes; these are frequently used to produce liquid fuels to power engines and generators.
Garcia-Perez et al. provide a useful review of biomass resources, collection methods, transportation considerations, and pretreatments such as drying and grinding in (Garcia-Perez, et al., 2012).

2.3.2 Biomass Properties

The suitability of a particular type of biomass for energy production is dependent on several of its properties including composition, heating value, density, and production yield.

One method of characterizing biomass composition is proximate analysis, which measures moisture, volatile matter, fixed carbon, and ash content by thermogravimetric analysis (TGA). Moisture, defined as mass lost upon heating to just above water's boiling point, typically 105°C, represents weight that does not contribute to energy value. Because weight basis can have such large implications for transport, storage, and biomass conversion, it is important to specify whether moisture content is reported on a wet or a dry basis (Quaak, et al., 1999). Dry weight percent is most commonly used to avoid confusion from large variations in moisture content from one sample to another and over time. Volatile matter is typically defined as the portion of biomass that decomposes into the gas phase under heating in an inert environment. This value is important for designing biomass burners and other thermochemical processing unit operations, especially in relation to the fraction that does not volatilize in an inert environment, i.e. the fixed carbon. Samples with low volatile matter content do not ignite easily (this is why lighter fluid is often needed to start a charcoal barbeque). Ash is composed of the inorganic minerals contained in the plants and any soil contaminating the biomass. Like moisture content, ash represents weight that does not contribute to energy value. In proximate analysis, ash is defined as any material remaining after the sample is combusted in air, usually at temperatures around 750°C.

Another method for characterizing biomass composition is elemental analysis (CHN, CHNO or CHNSO) or ultimate (CHNSO plus Cl) analysis. C and H generally contribute to energy content, while N, O, S, and Cl generally detract from energy content and can lead to emissions problems (Brown and Brown, 2014, Quaak, et al., 1999).

Biomass energy content is usually reported as higher heating value (HHV). HHV is the enthalpy released when a fuel reacts with oxygen under isothermal conditions; this measurement assumes the water vapor formed during the reaction is not condensed at the end of the process. Lower heating value (LHV) may also be reported. LHV is defined in the same way as HHV except LHV does not include the latent heat of produced water condensation. HHV is measured directly

by oxygen bomb calorimetry. It can also be estimated from correlations using proximate, ultimate, or biochemical composition analyses (Annamalai, et al., 1987, Channiwala and Parikh, 2002, Cordero, et al., 2001, Jiménez and González, 1991, Kim, et al., 2014, Quaak, et al., 1999, Shajizadeh and Degroot, 1976, Sheng and Azevedo, 2005, Tillman, 1978).

There are two important kinds of density for evaluating biomass as an energy source: bulk density (kg/m^3), and energy density or volumetric energy content (GJ/m^3). These two densities are related by HHV and are critical for biomass handling and transportation logistics; the lower the energy density, the more vehicle space is required to transport a given amount of energy. The bulk density of herbaceous biomass typically ranges from 50-200 kg/m^3 while that of woody biomass typically ranges from 200-500 kg/m^3—well below the densities of fossil fuels (~600-900 kg/m^3). Table 2.1 shows bulk and energy densities for several kinds of fuel. Cellulose is the only plant component with a consistent HHV (~18 MJ/kg) due to its well-defined chemical structure. HHV for lignin varies over a range of 23.3-25.6 MJ/kg (Sheng and Azevedo, 2005). In general, biomass that contains more lignin has a higher energy density than biomass that is mostly carbohydrates.

Table 2.1. Energy content and densities of different fuels (Brown and Brown, 2014, Erol, et al., 2010)

Fuel	HHV (MJ/kg)	Bulk Density (kg/m^3)	Energy Content (GJ/m^3)
Diesel	46	850	39.1
Gasoline	48.24	740	35.7
Coal	18.33-36.67	600-900	11-33
Hardwood	18.92-18.95	280-480	5.3-9.1
Softwood	20	200-340	4-6.8
Agricultural residues	16-18	50-200	0.8-3.6
Nut shells	20.31	64	1.3
Animal manure	17.36	400	6.944
Municipal solid waste (MSW)	19.87	--	--
Orchard prunings	19.05	--	--
Sunflower shells	17.86	64	1.143
Methanol	22.27	790	17.6
Ethanol	29.74	790	23.5
Biomass pyrolysis oil	8.28	1280.2	10.6

2.3.3 Biomass Densification

One pretreatment method used to overcome the challenges of biomass energy is densification. Densification can increase the bulk and energy densities of biomass

by as much as 10 fold. It can also improve particle size and shape homogeneity, and particle durability, making biomass much easier to transport, store, and handle. Densification can be performed with a variety of equipment including pellet mills, screw extruders, briquette presses, cubers, roller presses, tablet presses, etc.; the first three are the most common methods. Energy consumption and end-product quality differ depending on the densification method. For example, screw extrusion has the highest energy consumption since it shears and mixes the material in addition to compressing it. A hardwood or softwood feedstock with an 8% of moisture content, 2-6 mm particle size, and bulk density of 200 kg/m^3 fed through a screw extruder can reach a bulk density of 1400 kg/m^3 while its moisture content decreases to 4% (Shastri, et al., 2014, Thoreson, et al., 2014, Tumuluru, et al., 2011). Densification end-product quality grades are often determined based on particle size uniformity, durability index, heating value, and moisture, ash, and chloride contents (2011). For some applications, quality certification programs are available. In the case of wood pellets for residential and commercial heating, the common standards are the ENplus quality scheme, the CANplus quality scheme, and the Pellet Fuels Institute (PFI) Standards Program, in the E.U., Canada, and the U.S., respectively (Wiberg, 2014). Recent research has focused on expanding the biomass densification market past wood pellets made using pellet mills and standard operating parameters. Adapa et al. (Adapa PK, et al., 2002, Adapa PK, et al., 2003), Ndiema et al. (Ndiema, et al., 2002), Li and Liu (Li and Liu, 2000), and Mani et al. (Mani, et al., 2006) have studied the pelletization of agricultural straw, the effects of die pressure (20-140 MPa) on biomass relaxation characteristics, high pressure (34-138 MPa) densification of wood residue, and compaction characteristics of lignocellulosic biomass using an Instron Universal Testing Machine, respectively. Pretreatment processes such as steam explosion, grinding, and torrefaction can be used to decrease densification energy consumption and improve biomass binding. Sarkar et al. showed that the bulk density of switchgrass could be increased from 138 kg/m^3 to 499 kg/m^3 through densification alone, and up to 598 kg/m^3 when densification followed torrefaction at 270°C (Sarkar, et al., 2014).

2.3.4 Extracting Energy from Biomass

Due to the exothermic characteristics of carbon-carbon and carbon-hydrogen bond oxidation, lignocellulosic biomass may be burned directly as a solid fuel for process heat, or converted to flammable gases and liquids for later use. There are two broad conversion technology platforms: biological/biochemical and thermochemical/catalytic. The biological/biochemical conversion platform includes hydrolysis, fermentation, anaerobic digestion, and composting; this platform will not be considered here. The thermochemical conversion platform includes gasification, pyrolysis, and torrefaction, (as well as hydrothermal liquefaction (HTL) and solvolysis, which are not considered here).

2.3.4.1 Combustion

Biomass direct combustion is the complete oxidation of biomass at moderate to

high temperatures to produce hot flue gas and ash. The hot flue gas, mostly carbon dioxide and steam, can be used for many applications such as drying and space heating (low pressure), and power generation (high pressure). Combustion furnaces can be direct-fired or indirect fired. In direct-fired furnaces, the fuel is burned in the process steam or the process stream is in direct contact with the flue gases. This contact makes it probable that the process steam will become contaminated by combustion products (tars, ash, etc.) In indirect-fired furnaces, the combustion products are somehow separated from the process stream, such as with thermally conductive walls or with air-to-air heat exchangers.

Furnaces are often integrated with boilers for steam production. The two most common boiler configurations are fire-tube boilers and water-tube boilers. Fire-tube boilers, in which combustion gases are passed through tubes inside a water vessel, are more suitable for gaseous or volatile liquid fuels. Water-tube boilers, as the names implies, pass water through tubes held inside the fire; water-tube boilers are more complex and are more suitable for solid fuels, such as biomass (Brown and Brown, 2014). Solid fuel furnaces/water-tube boilers can be grouped into grate-fired, suspension, and fluidized bed systems. Grate-fired system combustion efficiency is barely more than 90% due to mass transfer limitations, while the efficiency of the other two systems can exceed 99%. Suspension burners are equipped with pulverizers to reduce the particle size of the fuels and enable entrainment for efficient conversion; their wide-spread implementation, however, has been hindered by their large NOx emissions caused by high operating temperatures. Fluidized bed burners, due to their excellent mixing and large heat transfer surface areas, can operate at lower temperatures (~850°C) and thus limit their NOx emissions. Whole tree burners also exist and can decrease wood harvesting and handling costs by eliminating the need for wood chipping (Brown and Brown, 2014).

The biomass combustion reaction consists of four stages: 1) warming and drying, 2) pyrolysis, 3) flaming pyrolysis, and 4) char combustion. Oxygen is only needed for the third and fourth stages. The warming and drying stage is endothermic and results in the evolution of associated water. As the temperature increases past 200°C in the second stage, hemicellulose and lignin begin to decompose and volatilize (i.e. pyrolyze). As the volatile gases from pyrolysis exit the biomass particle, they come in contact with oxygen which can result in gas phase reactions to form a flame, H_2O and CO_2. Once the gas phase reactions (third stage) are complete and oxygen can reach the surface of the biomass char remnants, solid-gas oxidation (fourth stage) reactions take place. Depending on the availability of oxygen and char temperature, the produced CO may be oxidized to form CO_2 (Brown and Brown, 2014).

Further information about biomass combustion can be found in (Branca and DiBlasi, 2003, Jenkins, et al., 1998, Zanzi, 2001).

2.3.4.2 Gasification

Gasification is simply combustion at slightly lower temperatures (750-1500°C) with less than the stoichiometric amount of oxygen, forming carbon monoxide and hydrogen (synthesis gas or "syngas") rather than carbon dioxide and water. Gasification has been in use since 1812 in England, when conversion of coal to gas was needed for illumination purposes (lamps fueled by "town gas"). Syngas is flammable and includes small amounts of CO_2, CH_4, H_2S, and NH_3. If syngas contains a significant amount of N_2 from using air as the oxidant, it is called producer gas. Syngas/producer gas can be used for thermal energy generation in much the same way as natural gas, and as a material feedstock for making liquid fuels and other chemicals. Biomass' high volatile matter content (70-90%) compared to many coals (30-40%), and the high reactivity of biomass char, make biomass a suitable feedstock for gasification (Zanzi, et al., 2002). Two challenges when designing biomass gasification reactors are how to treat incompletely-reacted tars, and how to avoid sintering and other reactor damage from the ash fraction (Quaak, et al., 1999). More information on biomass gasification, syngas cleaning and conditioning, and follow-on reactions can be found in (Chen, et al., 2003, Matsuoka, et al., 2008, Skoulou, et al., 2008, Timmer, 2008, Vigouroux, 2001).

2.3.4.3 Pyrolysis and Torrefaction

Pyrolysis is the heating and decomposition of biomass in the absence or severe limitation of oxygen to create a distribution of different products. Pyrolysis can be thought of as just the first two stages of combustion. Torrefaction is low temperature pyrolysis (200-300°C) used as a pretreatment to remove water and easily-degradable compounds while increasing biomass friability and energy density (Park, et al., 2014, Zanzi, 2001). Pyrolysis can be categorized into slow pyrolysis and fast pyrolysis where slow and fast refer to the heating rate (~10°C/min in slow pyrolysis and >500 °C/s in fast pyrolysis) and relative reaction time. Slow pyrolysis is the long-used technology for producing charcoal; its operating conditions maximize solid yield (Zanzi, 2001). Fast pyrolysis uses kinetic controls to optimize the liquid product yield. Both types of pyrolysis are usually conducted at 400-600°C, although slow pyrolysis may be done at lower or higher temperatures to adjust char properties. Biomass pyrolysis products include all three phases: gases (mostly CO, H_2, CO_2, CH_4, C_2H_2, etc.), liquids (bio-oil/tar and water), and solids (biochar and/or ash). The distribution of products changes depending on the biomass used and the operating conditions; a decrease in bio-oil yield results in an increase in biochar and gas yields, and vice versa.

Non-condensable pyrolysis gases can be the product of primary biomass decomposition, as well as the product of secondary tar cracking and char gasification. Gas production is typically favored by higher temperatures, longer reaction times, and smaller particle sizes (Zanzi, 2001). Although pyrolysis gas has a low heating value, it is still suitable for thermal energy production and power generation (Chen, et al., 2003, Park, et al., 2014). In a characterization study of pyrolysis gas, Brown et al. showed that carbon monoxide, carbon

dioxide, nitrogen, and methane contributed the highest concentrations, respectively (Brown, et al., 2011). Besides these gases, oxygen and traces of ethylene, ethane, propylene, and C4 gases were also observed. The heating value increased from 8 to 15 MJ/kg as the pyrolysis temperature increased from 525 to 650 °C, with carbon monoxide and methane providing nearly 80% of the gas heating value (Brown, et al., 2011). For rice straw pyrolysis, Park et al. also found an increase in gas heating value with temperature: from 4.1-11.4 MJ/kg over 300-700°C, respectively (Park, et al., 2014).

Biochar is the carbon-rich solid product of pyrolysis that can be used as a solid fuel, a feedstock for activated carbon adsorbent production, and as a soil amendment to improve soil fertility and sequester carbon (Brown, et al., 2011). Yields of biochar are usually 15-20% for fast pyrolysis and 20-50% for slow pyrolysis on a dry biomass weight basis. Lignin content in biomass typically favors char formation reactions resulting in higher char yields (Brown, et al., 2011, Lee, et al., 2010, Lee, et al., 2013). For a temperature range of 450-500°C, slow pyrolysis produces about 0.26 kg of char per kg of biomass, with approximately 45% of the biomass carbon being retained in the char (Shabangu, et al., 2014). Biochars usually have HHVs similar to those of coals (13-23 MJ/kg), where slow pyrolysis and woody feedstocks favor higher HHVs compared to fast pyrolysis or gasification and herbaceous feedstocks (Brewer, et al., 2009).

2.4. Energy and Water Desalination

2.4.1 Energy Requirements for Desalination

Water desalination plants use about 4-20 kWh/m^3 (14-72 MJ/m^3) of electrical energy equivalent to produce fresh water; if thermal energy has to be converted to produce electrical energy (at ~30% efficiency), this value would be approximately 46-240 MJ/m^3 (Al-Karaghouli and Kazmerski, 2013). Desalination unit energy consumption contributes about 60% of water production costs (Al-Karaghouli and Kazmerski, 2013). For an energy optimized desalination system, Semiathas showed that the energy costs can be decreased to 30-44% of total water production costs (Semiat, 2008).

The amount of energy needed for water desalination is dependent on many factors such as the form of energy (electrical, thermal, etc.), plant capacity, plant design configuration, and feed water TDS. The energy needed for MED and MSF processes is generally much higher than that required for RO because of the water evaporation step in MED and MSF, and significant improvements in RO technology that have lowered its power consumption (Fiorenza, et al., 2003, Kalogirou, 2005). Thermal desalination technologies, however, are capable of decreasing the TDS to less than 10 ppm while RO technologies can reduce the TDS to 10 ppm to 500 ppm, depending on the membranes used. The TDS limits for drinking water are typically 400 to 500ppm—much higher than that of water produced in MED and well within the range for RO (Al-Karaghouli and Kazmerski, 2013). For drinking water, therefore, some untreated feed water can

be added to the desalinated water to moderate the TDS concentration and make MED water more cost-effective (Sen, et al., 2013).

Water desalination plant capacities, energy requirements, and produced water costs for small-scale plants are shown in Table 2.2. As expected, energy and cost requirements for small-scale plants are much higher than those for large-scale plants. All of the energy requirement values assume that chemical energy from biomass is converted to thermal energy and that thermal energy is converted to needed electrical energy at an efficiency of 30% to account for thermodynamics. For example, if 1 kWh/m^3 (3.6 MJ/m^3) of electrical energy was described in the original reference, the table will list 12 MJ/m^3 of thermal energy.

2.4.1.1 Energy Consumption in RO

A typical RO unit, with an energy recovery system and a plant capacity of up to 128,000 m^3/day for seawater and 98,000 m^3/day for brackish water, consumes 14.4-21.6 MJ/m^3 (4-6 kWh/m^3) and 5.4-9 MJ/m^3 of electrical energy, respectively. This difference in energy requirements is the main cost difference between treating seawater and brackish water by RO (Semiat and Hasson, 2012). High TDS concentrations result in more energy consumption at a rate of approximately 3.6 MJ/m^3 (1 kWh/m^3) per 10,000 ppm (Garcia-Perez, et al., 2012).

2.4.1.2 Energy Consumption in MSF

The factors that affect energy consumption in MSF systems are temperature of the heat sink, number and geometry of the stages, feed water TDS concentration, unit construction materials, and heat exchanger configuration. Increasing the GOR, the number of stages, and the heat transfer surface area are all ways to lower energy consumption (Al-Karaghouli and Kazmerski, 2013, Elimelech and Phillip, 2011, Miller, 2003, Semiat, 2008). From design information provided by commercial manufacturers, a typical MSF, with a production rate of 50,000-70,000 m^3/day and a GOR of 8-12, consumes between 190 MJ/m^3 and 282 MJ/m^3 of thermal energy, and 13.5 MJ/m^3 (3.75 kWhe/m^3) of electrical energy (Al-Karaghouli and Kazmerski, 2013, Semiat, 2008).

2.4.1.3 Energy Consumption in MED

Similar to MSF, MED needs thermal energy for water evaporation and electrical energy to power pumps. A typical MED unit, with a production rate of 5,000-15,000 m^3/day, a top brine temperature (TBT) of 64-70˚C, and a GOR of 10-16, requires 145-230 MJ/m^3 of thermal energy and 8.1 MJ/m^3 (2.25 kWh/m^3) of electrical energy. The energy consumption for both MSF and MED could be decreased significantly if they used cogeneration power plants, where waste steam from the power turbine exhaust provides the initial thermal energy (Al-Karaghouli and Kazmerski, 2013, Semiat, 2008).

2.4.1.4 Energy Consumption in VC

Mechanical vapor compression (MVC) only requires electrical energy. A MVC unit, with a production rate of 100-3,000 m^3/day and a TBT of 74˚C, requires 25.2-43.2 MJ/m^3 (7-12 kWh/m^3). A thermal vapor compression (TVC) unit, with a production rate of 10,000-30,000 m^3/day, a GOR of 12, and a TBT of 63-70˚C, requires 227.3 MJ/m^3 of thermal energy and 5.7-6.48 MJ/m^3 (1.6-1.8 kWh/m^3) of

electrical energy (Al-Karaghouli and Kazmerski, 2013, Semiat, 2008).

Table 2.2. Water desalination plant capacities, thermal energy requirements (assuming a 30% efficiency for conversion of thermal energy to electrical energy if electricity is required), and water production costs for small-scale (<100 m^3/day) conventional and renewable energy source-desalination technologies.

Method	Size (m^3/day)	Water	Energy (MJ/m^3) Electrical	Thermal	Cost (US$/$m^3$)	Ref.
Conventional MED (single-purpose)	<100	Seawater	-	-	2.0-8.0	(Al-Karaghouli and Kazmerski, 2013)
Diesel MED	4	Brackish	-	1,110	26.50	(Sen, et al., 2011)
Conventional RO	20-1,200	Brackish	-	-	0.78-1.33	(Karagiannis and Soldatos, 2008)
Solar Still	<100	-	0	Passive solar	1.3-6.5	(Al-Karaghouli and Kazmerski, 2013)
Solar Multiple Effect Humidification	1-100	-	18	355	2.6-6.5	(Al-Karaghouli and Kazmerski, 2013)
Solar MED	1	Brackish	-	-	25.3	(Al-Karaghouli, et al., 2009)
Solar MED	72	Seawater	-	-	3.6-4.35	(Al-Karaghouli, et al., 2009)
Solar Membrane Distillation	0.15-10	-	0	540-708	10.5-19.5	(Al-Karaghouli and Kazmerski, 2013)
Solar PV RO	<100	Seawater	48-72	0	11.7-15.36	(Al-Karaghouli and Kazmerski, 2013)
Solar PV RO	<100	Brackish	18-48	0	6.5-9.1	(Al-Karaghouli and Kazmerski, 2013)
Solar PV ED	<100	-	18-48	0	10.4-11.7	(Al-Karaghouli and Kazmerski, 2013)
Wind RO	19	Seawater	-	-	4.4-7.3	(Al-Karaghouli, et al., 2009)
Wind RO	12	Seawater	-	-	2.6	(Al-Karaghouli, et al., 2009)
Wind MVC	<100	-	84-144	0	5.2-7.8	(Al-Karaghouli and Kazmerski, 2013)
Geothermal MED	80	-	24-36	149-289	2.0-2.80	(Al-Karaghouli and Kazmerski, 2013)

2.4.2 Fossil Fuel Energy and Water Desalination

Conventional water desalination technologies, especially those with the highest capacities in the Middle East, are powered by fossil fuels such as coal, crude oil,

and natural gas. Concerns about future availability, greenhouse gas emissions, and environmental impacts of fossil fuels has helped focus future water desalination technologies (and power generation in general) towards energy efficiency and renewable energy (Nisan and Benzarti, 2008).

Nisan et al. showed that, at present coal prices, the integration of RO or MED water desalination systems with circulating fluidized bed, coal-fired power plants would result in the lowest power and desalination costs, while oil-fired power production would result in the highest desalination costs. From an environmental impact analysis perspective, RO with a combined cycle gas turbine power plant had the lowest emissions of NO_x, SO_x, CO_2, and particulates, while MSF with a coal-fired power plant had the highest emissions (Nisan and Benzarti, 2008). Methnani has shown that RO water desalination, coupled with any type of fossil fuel, would have lower costs than MED due to the lower energy requirements for RO. This difference in costs, however, is generally negligible except when treating very high salinity water (Methnani, 2007). The use of pulverized coal rather than lump coal in power plants results in higher efficiency for the boiler (and the whole desalination system) since more of the furnace volume is used and the coal is more completely combusted (Tian, et al., 2005).

2.4.3. Renewable Energy and Water Desalination

The integration of renewable energy with desalination is especially suitable for remote areas and areas lacking connection to electrical energy grid infrastructure; in some cases, solar is the only feasible option due to distance from other resources (Al-Karaghouli, et al., 2009, Tzen, 2005). The most popular renewable energy sources for water desalination units have been solar photovoltaic (PV), solar thermal, wind, and geothermal, and hybrids of these options. Factors to consider when pairing renewable energy and desalination technologies include type, amount, and cost of energy available, site topography and geographical conditions, plant size, feed water salinity, capital costs, treatment requirements, and local infrastructure. 13% of renewable energy powered desalination systems worldwide are solar-MED, while 6% are solar-MSF. Eltawil et al. provide a very useful table of combinations of renewable energy sources and water desalination methods in (Eltawil, et al., 2009).

2.4.3.1 Solar Energy and Water Desalination

Solar energy may be used for water desalination unit indirectly, such as by connecting a solar collector to a desalination system, or directly, such as within a solar still where collection and desalination occur in a single unit.

Both MED and MSF can be used with solar collectors providing steam. The first method is direct steam generation (DSG), which uses parabolic trough collectors and fresh water, brine, or seawater as the heat transfer fluid (García-Rodríguez and Gómez-Camacho, 2001). In a solar DSG-MED system, the solar collector plays the role of the first effect: feed water, pre-heated in the MED, enters the solar collector and is partially evaporated by solar energy. The steam generated in the collector is then used as the heat source in the second effect. In such a system,

the initial steam is generated from the feed water/brine rather than fresh water (García-Rodríguez and Gómez-Camacho, 1999); however, fresh water may also be used for steam production (García-Rodríguez, et al., 1999). The second method for steam production in solar-MED systems also uses parabolic trough collectors but uses oil to transfer heat to the first effect. The third method for steam production is flashing pressurized water in a flash drum after it has been heated in the solar collector. Depending on climate conditions, any of these three methods may be used to enhance fresh water production (García-Rodríguez and Gómez-Camacho, 2001, García-Rodríguez, et al., 2002, Kalogirou, 2005, Qiblawey and Banat, 2008).

For direct solar water desalination, a conventional solar still uses a blackened bottom surface to absorb solar energy and the green-house effect to evaporate salty water within a V-shaped glass envelope. Solar still efficiency, the ratio of energy utilized in water evaporation to the solar energy incident on the glass cover, has a maximum value of approximately 35%. For more information on solar stills, see (Daniels, 1974, Eibling, et al., 1971, Kalogirou, 2014, Kalogirou, 2005).

Raluy et al. observed that for MSF units integrated with solar thermal energy, 63% of airborne emissions, including CO_2, NO_x, SO_x, and non-methane volatile organic compounds, decreased compared to MSF units using conventional fossil fuel boilers. The use of solar energy, however, requires special raw materials for cell and panel production compared to other renewable energies and, therefore, has more environmental impacts. Also, solar energy is available just part of the day (about 25% of the time) and thus, the cost of water produced through solar desalination is higher than that of water produced through conventional energy-powered desalination (Raluy, et al., 2005).

2.4.3.2 Hydroelectric Energy and Water Desalination

Hydropower is generated from the gravitational potential energy stored in water by damming rivers. Low-temperature waste heat from a hydropower turbine can be used as the thermal energy source for MSF and MED. Hydro-MSF has been shown to be the most effective combination in terms of reducing airborne emissions (79% decrease) compared to fossil fuel-MSF; the results were similar (71% emissions decrease) for hydro-MED (Akash and Mohsen, 1998, Murakami, 1994, Raluy, et al., 2005).

2.4.3.3 Wind Energy and Water Desalination

Wind, the result of atmospheric pressure differences caused by solar energy, is a suitable energy source for powering desalination units, especially for remote areas with high wind speeds such as islands (Kalogirou, 2005, Kiranoudis, et al., 1997). Because of weather-related wind speed fluctuations, efficient back-up power systems such as diesel generators, batteries, or flywheels are needed to stabilize the energy production rates (Tzen and Morris, 2003, Tzen, et al., 1998). One significant advantage of wind energy is its low cost compared to other renewable technologies. Wind is locally available and does not require much water transportation from treatment location to end user. Wind turbines can be coupled

with several desalination technologies, though they have mostly been used with RO systems. The amount of treated water that can be produced effectively by a wind-RO system is 50-2,000 m^3/day (Al-Karaghouli and Kazmerski, 2013, Eltawil, et al., 2009). A useful overview of wind energy has been provided by Ackermann (Ackermann and Söder, 2002). More information on wind-powered desalination is available in (Al-Karaghouli, et al., 2009, García-Rodríguez, et al., 2001, Habali and Saleh, 1994, Kiranoudis, et al., 1997, Lenzen and Munksgaard, 2002, Ma and Lu, 2011, Miranda and Infield, 2003, Robinson, et al., 1992).

2.4.3.4 Geothermal Energy and Water Desalination

Geothermal energy is heat stored beneath the earth's surface. Geothermal reservoirs can be low temperature (<150˚C) or high temperature (>150˚C); temperature directly affects which applications can make use of the stored energy. Medium to high temperature geothermal reservoirs can provide energy for either membrane or thermal desalination processes. One advantage of geothermal energy is that there is no need for additional energy storage reservoir heat supply is continuous and predictable. Ophir showed that a geothermal-desalination plant would cost as much as a large multi-effect dual-purpose desalination plant (Ophir, 1982). As described in a report by Awerbuch (Awerbuch, et al., 1976), the first geothermal-desalination pilot plant was built in Holtville, California in 1972, funded by U.S. Bureau of Reclamation (Al-Karaghouli and Kazmerski, 2013, Eltawil, et al., 2009). Pilot-scale geothermal-MED plants have been designed and tested in France (Bourouni, et al., 1999) and southern Tunisia (Bourouni, et al., 2001); the evaporators and condensers for these units were made of polypropylene and the unit operating temperature was 60-90°C (Bourouni, et al., 1999). Sometimes, brine from geothermal desalination systems can be used directly as the feed water/heat source for thermal desalination, or even RO, if the membranes can withstand higher temperatures (60-90°C). If a geothermal reservoir can provide high enough pressure water, it can provide shaft energy for mechanically driven desalination processes (Barbier, 2002, Houcine, et al., 1999).

2.4.3.5 Biomass Energy and Water Desalination

The literature is nearly silent on biomass energy for water desalination. Eltawil et al. described the use of biomass for water desalination energy as not being "a promising alternative since organic residues are not normally available in arid regions and the growing of biomass requires more fresh water than it could generate in a desalination plant" (Eltawil, et al., 2009). For most situations, this conclusion is reasonable, especially when large water treatment capacities are needed, the feed is high salinity seawater, or the biomass is grown only for energy production. In situations where very small plant capacities are needed, where significant amounts of local agricultural, forestry, or urban biomass residues are available and underutilized, and/or where the feed water is of relatively low salinity, biomass use may be feasible alternative.

For example, in New Mexico in the southwestern U.S., the climate is warm to hot and semi-arid to arid, enabling agricultural production through irrigation with ground water. This ground water has varying levels of salinity, from fresh to brackish. Residues from agriculture including pecan orchard prunings and shells

(Lillywhite, et al., 2010), cotton gin trash (Isci and Demirer, 2007), and dairy manure, in addition to urban yard waste, are locally available. In this scenario, biomass might conceivably serve as the energy source for a farm-scale irrigation or neighborhood-scale drinking water thermal water desalination plant. Combustion, gasification, or pyrolysis could be used to directly convert biomass into thermal energy. A slow pyrolysis process would have the added advantage of producing a value-added biochar product that would be used as an adsorbent for additional water treatment or as a soil amendment for improved soil water use efficiency and fertility (Barrow, 2012, Laird, 2008, Lal, 2008, Lehmann and Joseph, 2009, Lehmann, et al., 2003).

2.5 Economics

2.5.1 Economics of Water Desalination Plants

The costs for a water desalination plants may be grouped into capital costs and operational costs. Capital costs are one-time costs and include direct construction costs, such as land, equipment, buildings, and wells/surface water intake and concentrate disposal infrastructure, and indirect construction costs. Operational costs are recurring costs and include fixed costs such as insurance and amortization (usually 0.5% and 5-10% of the total capital costs, respectively) and variable costs such as maintenance, labor, energy, chemicals, supplies, etc. For a typical seawater RO plant, capital costs and energy costs represent 37% and 44%, respectively, of the total costs. For a similar thermal desalination plant, the capital cost fraction is lower (32%) and the energy costs higher (50%) because of the higher energy requirement per cubic meter of produced water for thermal systems (Eltawil, et al., 2009, Fiorenza, et al., 2003).

Energy consumption and hence, the final produced water cost, is significantly reduced in thermal desalination units if the power source is dual-purpose, i.e. the turbine is directly integrated with the desalination unit so that low-temperature exhaust heat energy provides the primary steam for desalination (Ophir and Lokiec, 2005). For example, the produced water cost of a 6 million gallon per day (22,700 m^3/day) single-purpose MED unit would be 0.739 cents/gallon (1.95 US\$/m^3), while the produced water cost from a similar capacity dual-purpose unit would decrease to 0.330 cents/gallon (0.87 US\$/m^3). Use of corrosion-resistant materials for heat transfer surfaces also decreases the capital and long-term energy costs for thermal desalination processes due to reduced scaling (Eltawil, et al., 2009).

Fresh water produced in conventional (fossil fuel-powered) MED plants with capacities of >90,000 m^3/day costs approximately 0.52-1.01 US\$/m^3. As the capacity of the MED plant decreases to 12,000-50,000 m^3/day, the produced water cost increases to 0.95-1.95 US\$/m^3. The estimated produced water cost for an MSF plant with a capacity of 23,000-528,000 m^3/day is 1.75-0.52 US\$/m^3, respectively (Al-Karaghouli and Kazmerski, 2013).

2.5.2 Economics of Coupling Renewable Energy and Water Desalination

Although many forms of renewable energy are available for free or very low cost, there are often significant capital costs for renewable energy systems, which result in dramatically higher produced water costs, especially at the smaller scale (see Table 2.2). These costs can be decreased with continuous improvements in renewable energy systems and power-saving strategies. Currently, renewable energy-powered water desalination systems are economically feasible only in rural communities with no access to an electrical grid, and/or where solar and wind resources are abundant.

The water production cost for a concentrated solar power-MED system with a production capacity of about 5,000 m^3/day, a thermal energy requirement of 147-289 MJ/m^3, and an electrical energy requirement of 2.5 kWh/m^3 (9 MJ/m^3) would be 2.40-2.80 US$/$m^3$ (Al-Karaghouli and Kazmerski, 2013, Fiorenza, et al., 2003). A typical geothermal-MED system, with a capacity of 80 m^3/day, a 80-100°C energy source, and the same energy requirements as the concentrated solar power system, would have a water production cost of 2.00-2.80 US$/$m^3$ (Al-Karaghouli and Kazmerski, 2013). Solar PV-RO and PV-ED are promising technologies in terms of economics; the main disadvantages of these systems are the low availability (and therefore high cost) of large PV arrays (Eltawil, et al., 2009).

2.6 Small-Scale Water Desalination Technologies

Much of the world's water desalination capacity is large-scale, fossil fuel-powered, seawater desalination. In general, produced water cost increases as plant capacity decreases and renewable energy sources are used. Small-scale desalination systems and their economics, however, are very important for small, rural communities where the available water is brackish or contaminated.
Sen et al. have focused on designing small-scale desalination systems for rural communities in India to address such concerns (Sen, et al., 2013). They developed a micro-scale MED system, initially powered by diesel, with 3 effects, a FF arrangement, a GOR of 3.6, and a fresh water production rate of 11-12 L/hr. (0.27 m^3/day). The unit can decrease the TDS of the water from 750 ppm to <10 ppm, well below the required TDS for potable water (Sen, et al., 2011). In another series of studies on small-scale MED unit design and operating parameters, Sen et al. experimented with 3, 6 and 9-effect systems, vertical tube evaporators using falling film water flow, and parallel feed alternatives. They found that a steam flow rate of 30 kg/hr. at 4 bar, and a feed water flow rate of 100 kg/hr., were satisfactory to meet design goals. The produced steam from the boiler was 130-140˚C and the feed water was heated to 110-112˚C (Sen, et al., 2011, Sen, et al., 2011, Sen, et al., 2011). The 9-effect MED, at semi-optimized parameters, produced 4 m^3/day of distilled water and required approximately 1110 MJ/m^3 of thermal energy at a cost of approximately 26.5 US$/$m^3$ (assuming a diesel energy content of 43 MJ/L, a cost of 0.86 US$/L, and a density of 0.832 kg/L) (Sen, et

al., 2011). These very high energy and cost values are expected to decrease with improvements in boiler efficiency, insulation to prevent heat losses, and continuing adjustments to the heat exchangers. Long-term goals for this research include increasing ease of fabrication, decreasing costs, and incorporating biomass-derived energy to replace the diesel fuel.

Biomass, with its relatively high moisture, oxygen, and ash content, and low bulk and energy densities, is best suited for small scale applications as transportation costs increase quickly with increasing distances (Wright and Brown, 2007). As such, biomass makes a less-than-ideal energy source compared to fossil fuels and electricity. Non-food biomass, however, is abundant in many places in the form of agricultural residues, forestry residues, yard waste, construction wood waste, and municipal solid wastes (cloth, paper, cardboard, etc.) (Downing, et al., 2011). Many of these residues go underutilized in landfills, especially in rural areas where these is less pressure for waste valorization. For those rural areas that require small-scale water desalination, communities should consider biomass-powered water treatment systems; such systems may not represent optimized energy efficiency or costs, but they may allow communities to meet their needs with the resources they already have. Biomass should also be considered as a supplement to solar power during off-peak times.

Conclusions

Different kinds of renewable energy-powered water desalination methods and technologies are available. For most scenarios, using renewable energy sources is much more expensive than conventional energy sources due to high capital costs. Improvements in energy efficiency and renewable energy collection/conversion technologies has somewhat driven down these costs, and the environmental benefits of using renewable energy sources has helped shrink the overall advantages of conventional energy systems. Much more research is needed for optimized site-specific renewable energy-powered water desalination system design.

If biomass is to be a feasible energy source for water desalination, a small-scale thermal desalination system in a rural area with lower salinity (brackish) feed water and abundant waste biomass is the most promising scenario. The economics of such a system would be significantly improved if the energy conversion method can produce other valuable products such as biochar.

3. Design Parameters for Biomass Pyrolyzer-MED System

3.1 System Scale and Desired Qualities

The low energy density nature of biomass dictates that biomass for energy be used close to its source. Close, by many estimates, is within several tens of miles (km) (Wright and Brown, 2007). Therefore, a water desalination system using biomass residues for energy will need to be on the scale of a single farm or a co-op of farms or residences. Within those constraints, the designed system must also account for the amount of biomass available on a seasonal basis and/or from storage. If the water is needed year–round, then the biomass must also be available year-round. On the other hand, if the produced water is to be used for a short-term purpose, such as flushing salts out of the root zone prior to planting or irrigating salt-sensitive seedlings, the seasonality of biomass residue supplies must be matched to the needed times.

The design of this system was based on the available water and biomass residues in the Mesilla Valley region of southern New Mexico. Brackish water chemistry was modeled off of wells 2, 3, and 4 at the Brackish Groundwater National Desalination Research Facility (BGNDRF) at Alamogordo, NM. These waters ranged in total dissolved solids (TDS) from 3,450 to 6,400 mg/L and pH values from 7.0 to 7.8 (Munoz-Guerra, et al., 2011). Target biomass residues were pecan shells, pecan orchard prunings, cotton gin trash, and yard waste. Other abundant residues that might be considered for this region are invasive species, namely tumbleweed and salt cedar, and dairy manure.

The design process started with the thermal and electrical energy needs of the multiple effect distillation (MED) water desalination unit and worked backwards to determine the needed biomass feed rate. The target fresh water production rate was 1-2 m^2/day or approximately 50 kg/hr.; this rate is considered micro-scale for water desalination technologies. The process would be continuous flow, use unit operations that could be installed on a mobile platform such as a trailer pulled by a pickup truck or a semi and be operated by two people. All of the energy needed for the water desalination would come from the biomass with the exception of start-up energy that might come from propane, diesel, or electricity. The pyrolysis process would be energy self-sufficient. Other sources of energy might be used for biomass size reduction (splitting, chipping) and drying. The process would be clean such that the only products were fresh water, brine, biochar and carbon dioxide.

3.2 Unit Operations

3.2.1 Process Flow

The process flow consists of 12 unit operations:

1. Biomass is added to a *feed hopper*;
2. From the feed hopper, biomass enters the *auger slow pyrolysis unit* and is converted into chars, bio-oil (as vapors and aerosols) and non-condensable gases (NCG) through partial combustion of the biomass;
3. Chars are fed into a *char collection* container where some of the cooled flue gases are warmed before being recycled into the pyrolysis unit;
4. Bio-oil vapors, aerosols and NCG flow into a *furnace* where they are combusted with additional air to form carbon dioxide and water;
5. Heat from the combustion furnace heats water in a *boiler* to produce steam;
6. Steam from the boiler is fed through a *steam turbine* to produce electricity;
7. Low pressure, low temperature steam is fed into the *first effect of the MED unit* to provide process heat; condensed steam is recycled to the boiler or collected with the distillate;
8. Electricity from the turbine generator is used to power the *vacuum pump* and the *water pumps* (feed water, brine, and distillate) of the MED;
9. Brackish feedwater is preheated using the *condenser unit of the MED* then a *heat exchanger* connected to the warm flue gas stream exiting the combustion furnace;
10. Preheated feedwater is sprayed into the *effects* in a parallel feed arrangement, creating a falling film over horizontal heat transfer tubes and producing low-pressure steam that flows into the next effect;
11. Brine collected at the bottom of each effect is removed to *brine storage* or recycled into the *feedwater tank*;
12. Distilled water collected in the condenser is pumped through a valve into *fresh water storage*; the *valve* allows the diversion of the produced water into the feedwater if the electrical conductivity is too high.

3.2.2 Steam for the MED

The energy required for primary steam for the MED was calculated as follows assuming the use of two evaporation effects.

For steam flow rate = 23 kg/hr., pressure = 0.5 bar absolute (7.3 psia), and temperature = 81.3°C (178°F), the amount of energy released by the steam within the MED first effect as latent heat is:

$$Q_{total} = Q_{latent} = M_{steam} \times H_{vap} \quad (1)$$

where M_{steam} is the steam flow rate and H_{vap} is the latent heat of vaporization. From steam tables for saturated steam at 0.5 bar and 81°C, the enthalpy of condensation is 2306.3 kJ/kg, which results in an energy transfer rate:

$$Q_{latent} = 23\frac{kg}{hr} \times 2306.3\ kJ/kg = 53{,}045\frac{kJ}{hr} = 14.73\ kW \quad (2)$$

This amount of thermal energy is appropriate to produce approximately 55 kg/hr. of fresh water if 227 kg/hr. of brackish water (TDS = 1,000-3,000 mg/L) is fed into the effect.

In the case that the exhaust steam from turbine is superheated (to a temperature higher than 81°C for the same steam pressure) the amount of energy released by steam within the MED effect would be:

$$Q_{total} = Q_{sensible} + Q_{latent} = M_{steam} \times C_p \times \Delta T + M_{steam} \times H_{vap} \quad (3)$$

where C_p is the heat capacity and ΔT is the temperature difference between the superheated steam and saturated steam. The heat capacity of the steam was estimated for the steam using a standard temperature-dependent heat capacity model from Table C.1 of (Smith, et al., 2005).

3.2.3 Electricity for the MED

The electrical power requirements for the MED unit assumed that four unit operations would be needed with individual power requirements of:

- 2.2 kW for a vacuum pump to provide vacuum at approximately 0.1-0.2 bar within the MED unit;
- 58 W for the distillate pump;
- 58 W for the brine pump;
- 108W for the feedwater pump;

which results in a total electrical power requirement of 2.45 kW.

3.2.4 Aspen Plus® Simulation

Process simulation software, Aspen Plus®, was used to model the mass and energy balances associated with the pyrolyzer-MED interface unit operations based on the thermal and electrical power needs of the MED unit. The model included four continuous, steady-state unit operations: a furnace to combust the non-condensable gases (NCG) and bio-oil to produce hot flue gas, a shell-and-tube heat exchanger (boiler) to use heat from the flue gases to produce steam, a turbine to convert the steam to electricity, and a second shell-and-tube heat exchanger to use residual heat in the flue gas to preheat the MED feedwater. The complete process flow is shown in Figure 3.1. Simulations were first run on as individual blocks using results from other block simulations. Once input and output streams were near converging on individual block bases, the unit operation blocks were combined into one single process block and the simulations repeated until convergence was achieved.

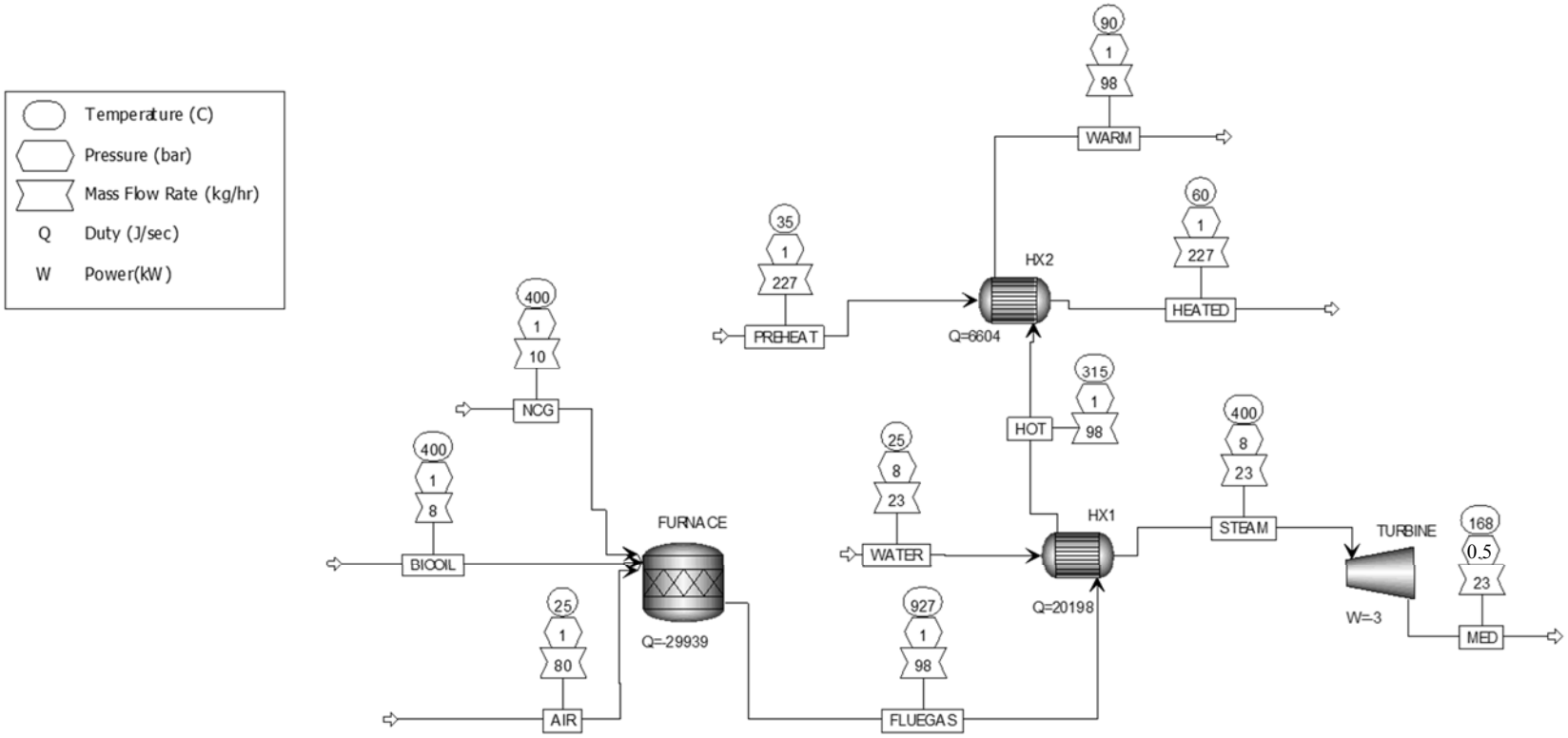

Figure 3.1 Aspen Plus® process flow diagram for pyrolyzer-MED interface showing stream temperatures, pressures, mass flow rates, heat duties and electrical power. HX1: heat exchanger 1, boiler; HX2: heat exchanger 2, preheater for the MED brackish feedwater; NCG: non-condensable gases; MED, multiple effect distillation unit.

3.2.4.1 Turbine Simulation

The only available option for a turbine in Aspen Plus® is the isentropic turbine. However, Aspen provides two temperatures for the outlet stream, one for the actual requirements and one for the idealized isentropic conditions, which are usually the same value initially. Turbine efficiency was set to the default value of 72%. The property method used was IAPWS-95, and the free-water phase properties were determined using STEAM-TA and water solubility method 3. The discharge pressure and indicated horsepower were 0.5 bar and 3 kW, respectively.

3.2.4.2 Boiler Simulation

From the turbine simulation preliminary results, the output requirements for the boiler heat exchanger were set to provide 23 kg of steam at 8 bar and 400°C. As with the turbine, the free-water phase properties were determined using STEAM-TA and water solubility method 3. The hot (steam) side of the boiler was modeled using Peng-Robinson vapor only; the cold (water) side was modeled using STEAM-NBS vapor and liquid. Heat exchanger configuration was set to countercurrent shell-and-tube with a minimum approach temperature of 1°C

3.2.4.3 Furnace Simulation

The furnace model was more complicated because NCG and bio-oil compositions and combustion reactions had to be specified. Using literature about slow pyrolysis NCG and bio-oil composition as guidance, five complete combustion reactions available in Aspen Plus® were selected in the following order:

$CH_4 + 2O_2 \rightarrow CO_2 + 2\ H_2O$

$2\ H_2 + O_2 \rightarrow 2\ H_2O$

$2\ CO + O_2 \rightarrow 2\ CO_2$

C_6H_5OH (phenol) + $7\ O_2 \rightarrow 6\ CO_2 + 3\ H_2O$

CH_3COOH (acetic acid) + $2\ O_2 \rightarrow 2\ CO_2 + 2\ H_2O$

The mole fractions for the NCG input stream were assumed to be 68% CO_2, 28% CO, 2% H_2 and 2% CH_4, at a temperature of 400°C and atmospheric pressure (Phan, et al., 2008, Wijayantia and Tanoue, 2013). The bio-oil input stream was set at 400 °C and atmospheric pressure with mole fractions of 53% phenol, 28.1% acetic acid, 9.2% furfural, 5.4% methyl acetate and 4.3% hydroxyacetone (Kim, et al., 2014, Phan, et al., 2008). Air was assumed to have a molar composition of 79% N_2 and 21% O_2 at an input temperature and pressure of 25°C and 1 bar, respectively. The property model used for the furnace calculations was Peng Robinson with free-water phase properties treated as ideal (due to the high temperatures and low pressures). The furnace efficiency was assumed to be 80% based on a standard gas-fueled boiler (2015). Furnace operation was optimized by varying the air flow rate and the combustion temperature. Input flow rates had to be adjusted when different heat duties were needed to avoid heat transfer

temperature cross over in the boiler.

3.2.4.4 Brackish Feedwater Preheater Simulation

The heat exchanger used to further cool the flue gas and to preheat the MED unit brackish feedwater was modeled as a countercurrent shell-in-tube exchanger. The cold side was modeled as liquid only using STEAM-NBS with an outlet temperature of 60°C; the hot side was modeled using gas-phase only Peng-Robinson. The minimum approach temperature was limited to 1°C.

3.3.4 Calculating Biomass Needs

The necessary flow rates of bio-oil and NCG from the pyrolyzer were calculated from the Aspen Plus® simulation of the furnace; from that calculation, the amount of biomass needed per m^3 of produced water from the MED unit can be estimated. In the slow pyrolysis of lignocellulosic biomass, approximately 60-70% of the dry feedstock mass is converted into bio-oil vapors and NCG, while the remaining 30-40% of the mass is converted into char (Lee, et al., 2013, Phan, et al., 2008). To get the amount of biomass needed, the combined mass flow rates from the bio-oil and NCG streams of the converged simulation were simply divided by the pyrolysis yields on a dry basis. Based on the bio-oil and NCG gas compositions assumed for the simulation, the combined bio-oil and NCG would have a higher heating value (HHV) of approximately 7.5 MJ/kg; with the 80% assumed furnace efficiency, 6.0 MJ/kg of this energy would be converted into usable energy for the boiler.

3.3 System Design Results

The results of the converged Aspen Plus® simulation are shown in Figure 3.1. The overall inlet streams into the furnace were 10 kg/hr. and 8 kg/hr. of NCG and bio-oil, respectively, at 400°C and 1 bar, and 80 kg/hr. of air. An optimum combustion temperature was calculated at 927°C and released 29.9 kW of thermal energy. The surface area needed for the boiler was 0.057 m^2 to produce 23 kg/hr. of steam at 400°C and 8 bars using 98 kg/hr. of hot flue gas at 1 bar and 927°C. Exiting the turbine was superheated steam at 168°C and 0.5 bar; the turbine produced 3 kW of work for an electrical generator. The surface area needed for the brackish water preheater was 0.06 m^2 and warmed 227 kg/hr. of brackish feedwater from 35°C to 60°C.

Assuming a 65% yield of bio-oil and NCG from slow pyrolysis, approximately 27.6 kg/hr. or 0.66 Mg/day of dry biomass is needed to produce 55 kg/hr. or 1.3 m^2 of distilled water. Put another way, approximately 475-550 kg of dry biomass is needed per m^3 of produced distilled water. Assuming a biomass purchase cost of US$50-75 per dry ton, treated water at this scale would cost 23-41 US$/$m^3$.

3.4 Conclusions and Future Research

Biomass contains enough energy to feasibly provide the energy for brackish water desalination using multiple effect distillation. The water production rates, unit operations and costs modeled here using Aspen Plus® represent the very low end

of small scale throughput, that is, what could be achieved in a laboratory-scale system. As expected at this scale, the produced water costs are approximately one order of magnitude higher than what could be achieved with economies of scale and an optimized number of effects. The mass and energy balances from the simulation demonstrate the proof-of-concept for a biomass pyrolyzer-MED system and provide a tool for designing real-world systems at different scales.

One challenge of pursuing a proof-of-concept prototype at such a small scale is the limited availability of optimized unit operations. For this system interface to be built for field testing, the scale will likely be selected based on the equipment available on the commercial market. Here, the steam turbine is likely to be the limiting equipment component, followed by the heat exchangers; the steam turbine should be selected first, then the simulation used to size the other components based on the available biomass feedstocks.

The cost estimate presented here is based on literature values for biomass purchase prices, such as in (Brown, et al., 2011), and does not consider capital and operating costs. The more likely scenario in the field is that the capital and operating (labor, maintenance, start-up fuel) costs will dictate the produced water cost while the biomass will be obtained onsite rather than being purchased. Future work with the developed simulation should be to add techno-economic analysis.

Three ways that the interface might be improved are the addition of water recovery from the biomass drying and combustion processes, the addition of heat exchanger to warm the boiler feed water using the superheated steam exiting the turbine, and the addition of an electrical air blower for the furnace to ensure adequate oxygen. Biomass from the field is usually wet and must be dried to less than approximately 10% moisture by weight prior to pyrolysis. A major product of combustion is water that currently is not recovered from the flue gas stream. Both sources of water represent opportunities to increase distilled water recovery rates. While the latent heat of the superheated steam might be used in the MED, the high temperature (168°C) would cause substantial scaling as the brackish water boiled in the effect; scaling is most likely at temperatures greater than 80°C. Since the boiler feed water does not contain salts, there is the potential for heat recovery without the risk of scaling. Finally, an air blower would give the furnace operator greater control over the combustion reaction to target an optimum temperature and increase combustion efficiency.

The interface modeled here assumes set rates and compositions of bio-oil vapors and non-condensable gases from biomass pyrolysis. Even though this model uses values that have been demonstrated in the literature, a complete design of a pyrolyzer-MED system will need to include pyrolysis reactor models that account for the variability with time inherent in pyrolysis reactions (start-up vs. steady state) and biomass composition. Such modeling is especially important for pyrolyzers that use direct heating through partial combustion of the biomass to provide the energy for the pyrolysis reactions, as anticipated to be the case here.

4. Producing Biochar from Locally-Available Biomass Resources

4.1 Lab-Scale Pyrolyzer Design and Fabrication

4.1.1 Pyrolysis Literature Review

Biomass pyrolysis is a thermochemical process that heats organic material to temperatures over 300°C in an oxygen-free environment to convert low energy density biomass into a high energy density oil (~22 GJ m^{-3} or ~17 MJ kg^{-1}), biochar (~18 MJ kg^{-1}) and syngas (~6 MJ kg^{-1}) (Bridgwater, et al., 1999, Ioannidou, et al., 2009). Biomass is composed of water, carbohydrates (cellulose, hemicellulose, starches, etc.), aromatic molecules (lignin), minerals (ash), and other compounds (extractives). The products of pyrolysis are 20–57% char, 32–58% oil, and 9-48% gas (Babu, 2008). Recently, more attention has been paid to biomass pyrolysis because pyrolysis can convert many types of organic material, such as municipal solid waste (MSW), agricultural waste, and forestry waste; and pyrolysis gas can be used for heating, power, and the creation of syngas, methane, hydrogen, etc.

As seen in the thermogravimetric analysis (TGA) results in Figure 4.1, there are significant behavioral differences between the three components of plant material. Cellulose starts decomposing at about 315°C and is mostly pyrolyzed by 400°C. On the other hand, hemicellulose is the first component in organic material to decompose, starting at 215-315°C but 20% hemicellulose is left unreacted in the solid residual, despite temperatures as high as 900°C. Lignin is the most difficult component to decompose with also the worst mass loss rate, leaving 47% by weight in the residual at 900°C (Fantozzi, et al., 2007, Yang, et al., 2007).

For biomass pyrolysis, there are three main stages (Fantozzi, et al., 2007):

1. Dehydration (25°C-100°C) removes moisture from the biomass.
2. Thermal cracking (100-350°C) decomposes biomass under oxygen free conditions. With the rise in temperature, a variety of volatile organic compounds (VOCs) will form, resulting in a loss of the majority of the original mass. Although the temperature reaches the ignition point of the material, the oxygen free conditions prevent the formation of a flame, as flame is gas phase oxidation reaction.
3. Carbonization (> 400°C) is generally considered to be caused by the further cracking of C-C and C-H bonds. Decomposition occurs very slowly in this stage and the resulting mass loss is much smaller than in the second stage. Biochar is formed when the C-C and C-H bonds in the VOCs are broken, dispersing them as gases.

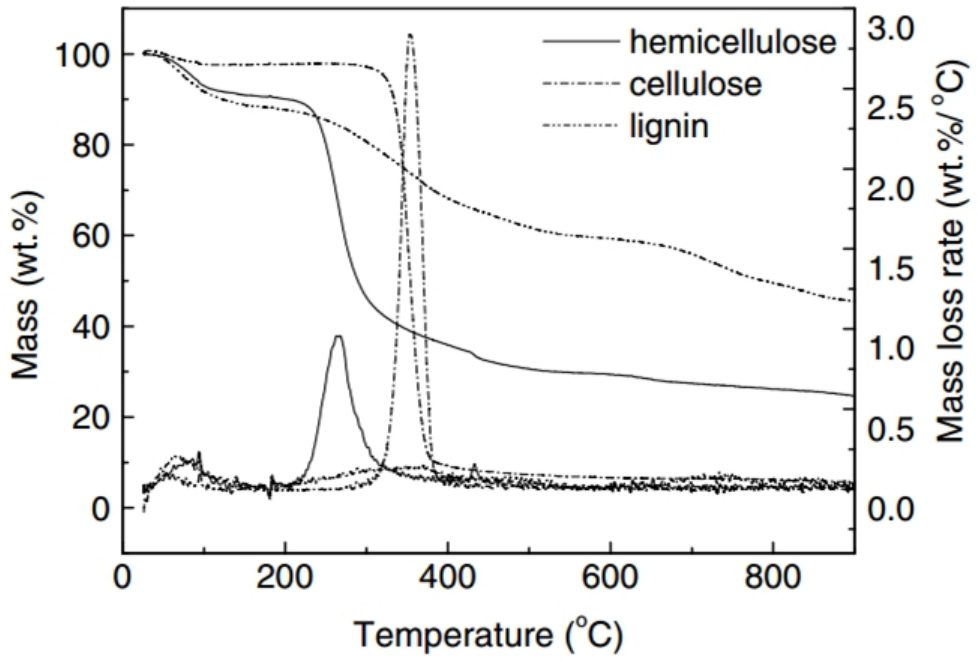

Figure 4.1. Pyrolysis curves of hemicellulose, cellulose and lignin in a thermogravimetric analyzer (Yang, et al., 2007).

Table 4.1. Parameters for different pyrolysis processes (Brewer and Brown, 2012).

Process	Residence time	Heating rate	Temperature range (°C)	Primary product
Carbonization	hours-days	Very slow	400-600	Biochar
Slow pyrolysis	5-30 min	Slow	350-600	Syngas, bio-oil, biochar
Fast pyrolysis	0.5-5 sec	High	650	Bio-oil

There are two primary methods of pyrolysis, slow pyrolysis and fast pyrolysis. These two methods vary in physical parameters like temperature, heating rate, residence time and primary products. Slow pyrolysis is mainly used to produce biochar from low-value biomass feedstock like yard waste, but can also be used to generate energy (Downie, et al., 2012). The heating rate is usually below 100 K/min, the reaction temperature range is from 300°C to 800°C, and the residence time varies from minutes to days. The yields of slow pyrolysis are roughly 35% biochar, 30% bio-oil, and 35% syngas by mass. Slow pyrolysis units are typically connected to an afterburner to burn the off-gases, often for heat or electricity generation (Brown, et al., 2011). Fast pyrolysis was developed from the slow pyrolysis process to maximize bio-oil production. It is operated at moderate temperatures with very high heating rates and short residence times. Several fast pyrolysis experiments have managed to convert 70-80% of the starting dry biomass weight into bio-oil (Winsley, 2007). The size and type of the pyrolyzer is

determined by the size of the feedstock. If the feedstock is too large, the heating rate will be too low to achieve fast pyrolysis. Typical particle sizes for fast pyrolysis are < 2 mm.

Table 4.2. Typical product yields (dry basis) obtained by different modes of wood pyrolysis (Winsley, 2007).

Mode	Conditions	Bio-oil	Biochar	Gas
Fast	Moderate temperature (500°C) for 1s	75%	12%	13%
Intermediate	Moderate temperature (500°C) for 10-20s	50%	20%	30%
Slow	Low temperature (400°C) with very long solids residence time	30%	35%	35%
Gasification	High temperature (800°C) with long vapor residence time	5%	10%	85%

4.1.2 Pyrolyzer Design Considerations

There are three main methods for heating pyrolyzers: direct heating, auto-thermal heating, and indirect heating. In direct heating, biomass, petroleum, or natural gas is burned outside of the pyrolyzer to generate hot combustion gases which enter the pyrolysis chamber and drive the pyrolysis reactions. In auto-thermal heating, some of the feedstock is burned/oxidized to generate the heat needed to pyrolyze the rest of the feedstock (Emrich, 1985). In indirect heating, hot gas flows through an external heating tube adjacent to the tube and heats the biomass by thermal conduction; this method ensures that pyrolysis will occur in an oxygen-free environment, but this also means that one must either recycle or remove the VOCs produced during pyrolysis. Figure 4.2 shows these various types of heating. In commercial applications, direct heating is usually chosen because it is cheap and easy to operate. In lab-scale applications, indirect heating methods give better control of the reaction temperature, heating rate, and residence time.

The batch reaction cycle includes a heating phase to create the biochar and a cooling phase to lower the biochar's temperature to prevent combustion upon exposure to air. Feedstock particles are kept stationary during the reaction while produced VOCs are released into the sweep gas. Semi-batch systems are more efficient at utilizing heat because the hot steam generated in one reaction cycle is reused in the next reaction cycle. Although some systems can also recycle liquid byproducts, most systems only recycle hot steam in producing biochar (Garcia-Perez, et al., 2010). In general, a continuous reaction chamber is operational 90-95% of the time because the reaction is only discontinued during the occasional maintenance of the chamber. Most reaction chambers are adjusted for continuous operation when the biomass feedstock flow rate is sufficiently high.

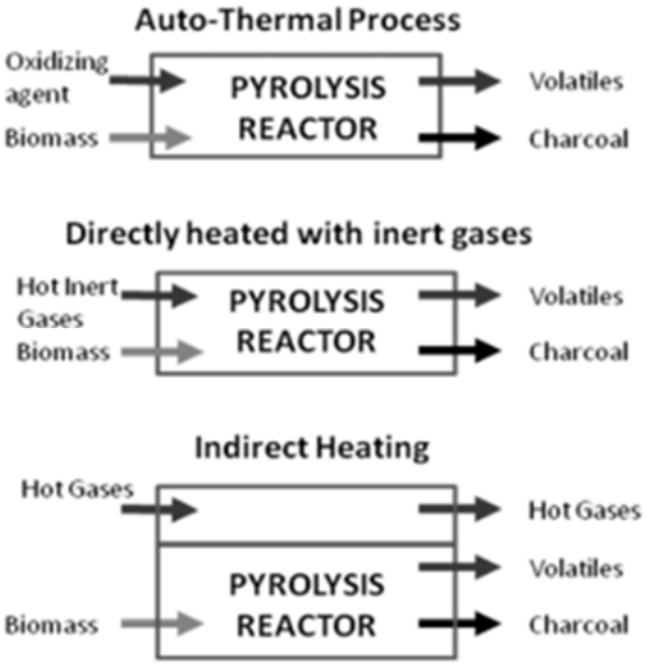

Figure 4.2. Types of pyrolysis heating methods (Garcia-Perez, et al., 2010).

Several lab-scale slow pyrolyzers have been developed for biochar research. The "buried sand" reactor was designed at Rice University to produce biochar for small-scale testing. Instead of using nitrogen as an inert purge gas, the entire reaction chamber was buried in 9 kg of sand, which allowed volatiles to escape through the sand and greatly limiting the diffusion of oxygen into the reactor. The reactor itself was a steel vessel covered by a loose-fitting porcelain lid containing the biomass (30-60g), glass wool and a thermocouple. Heat was provided by a box furnace with snorkel ventilation. This setup (thermocouple + furnace) gave the users good temperature control. Long wait times were common because the large mass of sand for heating and cooling. The sand insulation cannot be scaled to higher-yield applications because the mass, cooling time, and pressure generated by the sand. Nor was it possible to measure emissions due to the lack of an outflow collection mechanism (Kinney, et al., 2012).

The "meat smoker" reactor was a custom-built, pilot-scale batch reactor designed at Baylor University to produce large amounts of biochar using cheap, relatively common equipment including a truck-mounted, propane-powered pyrolyzer, and to collect bio-oils for further analysis. Biomass was sealed in a 20L soup pot coated with sealing grease. A custom lid and clamp kept the pot shut as the reactor was placed in a backyard smoker box equipped with an extra propane burner. The propane tank that was weighed before and after each reaction cycle (4 hours) to estimate energy usage. Each cycle produced roughly 2 kg of biochar. To remove VOCs, the lid contained a large vent connected to a series of large, air-cooled condenser tubes with openings at the bottom for bio-oil collection. Non-condensable gases were returned to and combusted in the second burner (Li, et al.,

2011). Despite its many advantages, this reactor did have a few problems. Reaction conditions were variable because temperature control was based on the imprecise dials of the smoker while the temperature of the biomass in the large pot was monitored by only one thermocouple. This often resulted in reaction temperatures above desired targets. The sealant also proved difficult to use and would sometimes fail.

The "paint can" reactor was designed at Iowa State University to produce slow-pyrolysis biochar for a biochar comparison study. A 0.95L (1 quart) paint can containing the biomass was placed inside a box furnace. An inflow line of nitrogen (1 L/min flow rate) and an outflow line for VOCs into an ice water impinger was included, as was a thermocouple for temperature measurement. A flow meter measured the gas outflow after non-condensable gases were cooled by the impinger (Brewer, et al., 2009). With relatively few parts, this system was cheap and easy to build. However, such a system required much maintenance: the outflow line often would clog because the tubing got too cold; this clogging created back pressure and sometimes fires in the lab furnace. The sealing material covering both ports would deteriorate after repeated heating cycles.

4.1.3 Design of Lab-Scale Slow Pyrolyzer

The goals of our pyrolyzer design were to produce relatively large amounts of reproducible biochar while managing VOCs and allowing for easy assembly, disassembly and cleaning. Integrated temperature control and VOC collection features are included. (Since we currently have no plans to analyze or recycle the produced VOCs, combustion would be the best approach. However, space constraints of the fume hood prevent the construction of a burner, so a condenser was built instead.)

The system consists of a GHA 12/450 single zone horizontal tube furnace (Carbolite, Hope Valley, UK) sized to fit a 5.5 in. (14 cm) O.D. 304 stainless steel reaction tube with a 1/4 in (6 mm) wall thickness. The programmable furnace provided an 18 in. (46 cm) heated zone for indirect heating. Inside the reaction tube, two circular 303 stainless steel plates with large holes were held in place with screws; 304 stainless steel 40-mesh wire cloth was placed between the plates on the biomass side to contain the biomass particles while allowing for gas flow. End caps for the reaction tube, with high temperature glass-mica ceramic O-rings, were held in place by clamps. One end cap contained openings for a thermocouple (Super OMEGACLAD XL, Omega) and a nitrogen gas inlet. A handheld data logger (OM-EL-ENVIROPAD-TC, Omega) was connected to the thermocouple to record the temperature of the biomass every 5 minutes. Pyrolysis vapors exited through the other end cap into a 0.95 cm O.D. tube maintained at 200°C by heat tape (XtremeFLEX BWH, BriskHeat Corp, Columbus, OH) with a temperature controller (SDC Digital Benchtop, BriskHeat Corp.) to prevent early vapor condensation and clogging. Vapors were bubbled through approximately 700 mL of distilled water in a large, glass Erlenmeyer flask set in an ice bath. The entire pyrolysis system was operated inside of a fume hood, as shown in Figure 4.3. The

fabrication process included cold-flow and hot-flow shakedown trials.

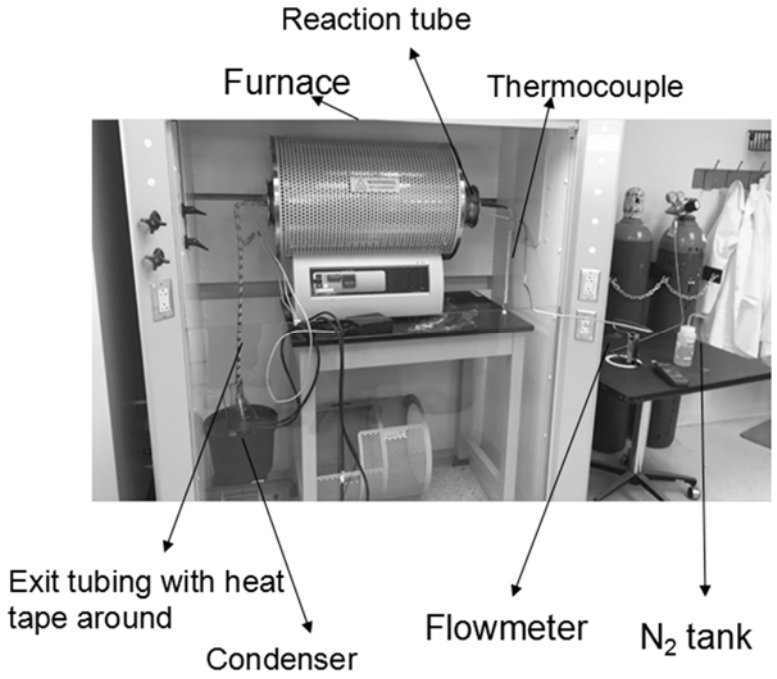

Figure 4.3. Custom-built lab-scale slow pyrolysis system used to produce biochar.

4.2 Biomass Feedstocks

Four feedstocks were selected for this study to represent underutilized biomass available locally. All feedstocks were air dried and stored in sealed buckets prior to pyrolysis.

Pecan (*Carya illinoinensis* (Wangenh.) K. Koch) orchard prunings were collected from the NMSU Leyendecker Plant Science Center in Las Cruces, NM. Prunings consisted primarily of small branches and twigs, with some leaf material.

Prunings were allowed to dry in the field, then were collected and chipped in a standard yard waste chipper. Pecan shells were collected from a local pecan processing facility and were used as received.

Cotton (*Gossypium hirsutum* L.) gin trash was collected from Mesa Farmers Coop - Cotton Gin in Vado, NM. The gin trash contained mostly cotton leaf and stem pieces, with noticeable amounts of lint and seed residues, and some other materials such as soil.

Yard waste was collected from the NMSU green waste yard on 17 April 2014. The waste consisted primarily of freshly cut and chipped wood waste from tree pruning around campus, with a small amount of mixed leaves, shrubs, and grasses collected from maintenance of xeriscaped areas.

4.3 Biochar Production

Biochars were produced from the four biomass feedstocks using the custom-built, lab-scale slow pyrolysis system. Biomass (200-250 g) was loaded into the reaction tube between the perforated plates. The furnace was heated at a rate of 5°C min^{-1} to 450°C and maintained at 450°C for 60 minutes, after which the furnace and heat tape were turned off and the system allowed to cool overnight. An inert atmosphere was maintained by flowing nitrogen gas through the reactor at a rate of 1.0 L min^{-1}. Once the biochar had cooled to room temperature, the reactor was disassembled and the biochar removed, weighed, and stored in sealed containers. Bio-oil yields were estimated from the change in mass in the water condenser; this yield did not include the non-trivial amounts of tar that had condensed inside the pyrolyzer and exit tubing. Non-condensable gas plus tar yield was estimated by difference. The reactor was cleaned by placing the reaction tube in the tube furnace without the end caps and heating the tube to 600°C for an hour to burn off tar residues.

4.4 Biochar Characterization

Moisture content of the biomass feedstocks and biochars was measured by heating ground samples in an oven at 105°C for 2 hours. Ash content was measured by heating 0.5 g of sample in a muffle furnace to 600°C and 750°C for 6 hours for biomass and biochar, respectively. Ash measurements were done in duplicate.

Higher heating values (HHV) of the biomass feedstocks and biochars were determined in duplicate using a Model 6725 semi-micro bomb calorimeter (Parr Instrument Co., Moline, IL). Mineral oil of known energy content was used as a spike for samples which did not easily ignite in order to ensure complete combustion.

4.5 Results

Pyrolysis product yields, and biomass and biochar characteristics are shown in Table 1. There was a lag of approximately 25-50°C during pyrolysis between the biomass temperature and the furnace set temperature due to heat transfer limitations; the actual highest heating temperatures were 433, 423, 425 and 419°C for pecan shell, pecan prunings, cotton gin trash, and yard waste, respectively. Biochars retained the particle size distribution and shape of the biomass feedstocks. Biochars were uniformly black in color, had little or no perceivable odor, and left no oily residue when smeared; these observations are consistent with complete biomass conversion. One exception was the cotton gin trash biochar, which had some interspersed dark brown particles, especially in the shape of the cotton lint residues, suggesting a slightly less severe pyrolysis intensity (Brewer, et al., 2012). The cotton gin trash feedstock also had a significantly higher ash content (12% on a feedstock weight basis, compared to 1-5%), which resulted in a higher biochar yield (42%, compared to 28-35%), higher

biochar ash content (31%, compared to 4-19%) and lower biochar HHV (24 MJ kg^{-1}, compared to 31-32 MJ kg^{-1}); these results indicate that the feedstock's mineral matter was concentrated in the biochar ash fraction. The biomass feedstock pyrolysis properties, yields, and higher heating values were consistent with other biomass slow pyrolysis processes. The collected bio-oil yields (11-18%) were lower, and the non-condensable gas (NCG) yields higher, than would generally be expected for this slow pyrolysis temperature since the tars coating the reactor and exit plumbing were not measured and thus were included in the NCG estimation.

Table 4.1. Yields of biochar, collected bio-oil, non-condensable gases (NCG) and uncollected tars from biochar production, reported on a wet feedstock basis. Moisture content, ash content, and higher heating values (HHV) of biomass feedstocks and biochars reported on a wet, unground basis; ± is standard deviation where n = 2.

Sample	Biochar Yield (wt. %)	Bio-oil Yield (wt. %)	NCG + Tar Yield (wt. %)	Moisture (wt. %)	Ash (wt. %)	HHV (MJ kg^{-1})
Pecan shell	--	--	--	5.8	1.4 ± 0.3	18 ± 0.5
Pecan prunings	--	--	--	5.7	2.7 ± 0.2	23 ± 3
Cotton gin trash	--	--	--	6.1	12 ± 1	17 ± 1
Yard waste	--	--	--	4.2	4.7 ± 0.3	22 ± 2
Pecan shell biochar	28	18	54	3.9	4.2 ± 0.1	31 ± 1
Pecan prunings biochar	35	13	52	4.3	10.8 ± 0.1	31 ± 2
Cotton gin trash biochar	42	11	57	3.3	31 ± 4	24 ± 3
Yard waste biochar	32	17	51	2.4	19 ± 2	32 ± 4

4.6 Conclusion

Biochar yields for 450°C slow pyrolysis of pecan shells, pecan orchard prunings, yard waste and cotton gin trash ranged from 28-42 wt.%, within the expected range for these conditions. From the characterizations available, these feedstocks and conditions produce biochars of acceptable quality for soil application; the CGT exhibited the high ash content and low HHV of feedstocks higher in mineral content which may impact its suitability for ash-sensitive applications.

5. Biochar Effects on New Mexico Soil Properties

5.1 Study Goals and Objectives

Soil quality is "the capacity of a specific kind of soil to function, within natural or managed ecosystem boundaries, to sustain plant and animal productivity, maintain or enhance water and air quality, and support human health and habitation" (Karlen, et al., 1997). Generally, arid soils have poor quality due to very low levels of soil organic matter (Idowu and Flynn, 2013). Organic matter is very central to the quality of any soil (Reeves, 1997). The organic matter levels of arid soils, particularly in New Mexico where this study was conducted, are often less than 1% (Ulery and Tugel, 1999); to improve the soil organic matter, considerable efforts are needed to add organic materials to the soil. Traditional ways for improving soil organic matter, such as cover cropping, leaving crop residues after harvest, and applying manure, are often difficult to achieve in arid soils due to water availability and salinity (Magdoff, 2001). For example, cover cropping has been very challenging for farmers in the arid desert southwest of the United States due to the reduced amounts of available water for agriculture (Idowu, et al., 2012). This region has suffered severe drought over several years and using scarce water for raising cover crops is perceived by many growers as uneconomical.

In order to improve soil organic matter of arid soils, innovative methods that will not compete with water for crop production need to be developed. One such innovative method is to convert locally available waste biomass materials into biochar for soil application. Biochar is a predominantly recalcitrant organic carbon (C) material, created when biomass is heated to temperatures between 300 and 1000°C under low oxygen concentrations (i.e. pyrolysis) (Jeffery, et al., 2011). Since the organic carbon produced in biochar is very stable, addition of biochar to the soil has the potential to both improve soil quality and sequester carbon, which is important for mitigation of excessive carbon dioxide in the atmosphere (McHenry, 2009).

Biochar application to the soil has been shown by different studies to have significant impacts on several soil quality parameters (Barrow, 2012, Laird, 2008, Lal, 2008, Lehmann, et al., 2003). Positive impacts of biochar amendment on soils include:

i) increasing soil capacity to sorb plant nutrients, consequently reducing leaching losses of nutrients (Cheng, et al., 2008, Liang, et al., 2006);
ii) decreasing soil bulk density, leading to less-compacted soil conditions favorable for root growth and water permeability (Laird, et al., 2010);
iii) increasing the soil cation exchange capacity (Steiner, et al., 2008);
iv) increasing soil microbial activity and diversity (Lehmann, et al., 2011, Steinbeiss, et al., 2009);
v) increasing plant available water retention (Karhu, et al., 2011, Laird, et al.,

2010); and

vi) increasing crop yields (Kimetu, et al., 2008, Steiner, et al., 2007).

From a biomass systems engineering perspective, using available biomass resources to meet the community's needs is critical to ecological sustainability. In arid agricultural communities, crop residues are often the primary available biomass feedstock and fresh water is often the primary need. Biomass can be used to help meet water needs in several ways, including providing the energy needed for water treatment. A way in which biomass for water treatment and biomass for soil amendments can be combined is to use slow pyrolysis to produce thermal energy for brackish groundwater desalination and biochars for application to agricultural soils.

New Mexico state usually ranks 3rd for pecan production in the United States with >17,000 pecan orchards covering more than 15,800 ha. Doña Ana County is New Mexico's highest pecan producing county at approximately 19,500 Mg yr^{-1} (Lillywhite, et al., 2010). Pecan production creates two residual biomass streams: pecan shells and pecan orchard prunings (leaves, branches, etc.). Estimates of the amount of pecan shells available from the New Mexico/western Texas pecan industries range from 14,000-26,000 Mg yr^{-1}; some of these shells have been used in the horticulture as a mulch and alternative potting media (Mexal, et al., 2003). Estimates of orchard pruning residues available from the Mesilla Valley region of New Mexico range from 11,000-37,000 Mg yr^{-1} on a dry basis. Air quality restrictions have caused pecan farmers to look for alternatives to conventional open-air pruning residue burning (Kallestad, et al., 2008).

After harvest and prior to textile production, cotton bolls must be ginned to remove the seeds (used to make cottonseed oil and cottonseed meal) and other non-lint materials. The non-seed, non-lint materials, such as stems, leaves and dirt, are collectively referred to as cotton gin trash. An average of 68 kg of gin trash is generated for each 218 kg bale of cotton. In 2013, approximately 12,000 ha of cotton were grown in New Mexico at an average yield of 0.89 bales/ha, resulting in over 725,000 Mg of cotton gin trash (unpublished cooperative extension service data).

Many municipalities collect tree branches, grass clippings, garden residues, and other yard wastes from residential and commercial properties for composting, mulching, and other uses. The City of Las Cruces, New Mexico (population approximately 100,000) receives 1,800-2,700 Mg yr^{-1} of wet green waste for processing into compost (Lisa LaRocque, City of Las Cruces Sustainability Officer, 23 September 2013). This represents a significant source of biomass that could be used for pyrolysis, especially for municipalities that are looking for alternative, higher-value uses for yard waste.

Pyrolysis of locally available waste biomass can help produce energy that can potentially be used for desalinization of increasingly salty well waters used for

irrigation and, at the same time, improve soil quality through the application of biochars. Therefore, the objectives of this study were:

- Assess the impacts of biochar amendments (derived from pecan shells, pecan orchard prunings, urban yard waste, and cotton gin trash) on multiple soil quality indicators in two different soil textures, sandy loam and clay loam.
- Assess the impacts of biochar amendments on soil water retention (moisture desorption) in two different soil textures, sandy loam and clay loam.

5.2 Soil Incubation Materials and Methods

Two local arid soils used for agriculture, a sandy loam and a clay loam, were amended with the biochars at a rate of 45 Mg ha^{-1}. The sandy loam soil (a Thermic Typic Torrifluvents (Staff, 1999)) was collected from the NMSU Fabian Garcia Agriculture Experiment Station in Las Cruces, NM. The clay loam soil (a Thermic Vertic Torrifluvents (Staff, 1999)) was collected from the NMSU Leyendecker Plant Science Center in Las Cruces, NM. Biochars were ground to pass a 2 mm sieve prior to addition to the soil. Soil samples were thoroughly mixed then packed into pots. Soils were first slowly saturated with water then allowed to drain for 24 h, after which they were placed into a growth chamber for 3 weeks. About 100 cm^3 of water was added twice a week to prevent the soil from drying out. The temperature of the growth chamber was set at a day temperature of 28°C and a night temperature of 20°C.

5.3 Soil Property Measurement Methods

Soil chemical analyses were conducted on the biochar-amended soils after incubation using standard procedures. The pH, electrical conductivity, calcium, magnesium, sodium, and sodium adsorption ratio of the soils were measured using the filtered solution from a saturated paste preparation (Laboratory, 1954). Soil organic matter (SOM) was measured using the Walkley-Black method (Nelson and Sommers, 1996). Sodium bicarbonate-extractable phosphorus (Olsen, et al., 1954) and potassium were measured by inductively coupled plasma (ICP) spectroscopy (Cihacek, 1983). Nitrate-N concentration was measured by water extract using a cadmium reduction column (Ludwick and Reuess, 1974). Copper, iron, manganese and zinc micronutrients were measured by DPTA extract and analyzed by ICP (Ludwick and Reuess, 1974).

The experimental design for the biochar soil amendment trial was a randomized complete block design, with treatment combinations replicated four times. Experimental treatments consisted of biochars from four different feedstocks [pecan shells (PS), pecan prunings (PP), yard waste (YW) and cotton gin trash (CGT)] and a control treatment with no biochar addition, tested in two soil types (sandy loam and clay loam), for a total of ten treatment combinations. Analysis of

variance was performed on soil measurements and the means of the treatment values were separated using the Student Newman Keuls test after a significant F-ratio.

Moisture desorption curves were used to assess the effect of biochar amendments on soil water retention in the plant available range, namely from field capacity (FC) at -33 kPa tension (336 cm or 132 in. of water, pF = 2.53 where pF = - log [h (in cm)]) to permanent wilting point (PWP) at -1,500 kPa tension (15,296 cm or 6,022 in. of water, pF = 4.19). Soil moisture desorption curves were measured using a HYPROP tensiometer system (UMS GmbH, Munich, Germany) and a WP4C Dewpoint potentiometer (Decagon Devices, Pullman, WA). The dewpoint potentiometer measures water potential in the based on measurements of humidity above a sample in a closed chamber.

Soil samples were prepared for tensiometer analysis by partially saturating them for several hours in their incubation pots, then inverting the pots onto a tray. The potentiometer sample ring was pushed over the sample and any soil sticking above the rim was gently pushed down to completely fill the sample ring. Excess soil was removed and saved for chemical analysis. The saturation base and a coffee filter were placed over the soil and the sample was completely saturated overnight. The HYPROP was run as per manufacturer instructions in multiple device mode with weight measurements taken 2-3 times per day until analysis runs were complete. Refilling was done overnight using a vacuum system that provided 850 kPa when connected to the HYPROP base. The HYPROP provides data in the wet range, from approximately -1 kPa (pF = 1) to -1,000 kPa (pF = 3).

To gain more information about the water capacity in the PWP range, samples from the HYPROP were removed as soon as the analysis was finished and analyzed using the dewpoint potentiometer according to manufacturer instructions. After each measurement, samples were allowed to air dry for a few hours then remeasured until the water potential was below the PWP. Soil dry weights were measured by drying in an oven at 105°C for 2 hours; these dry weights were then used to back calculate volumetric water contents of the soil samples for the dewpoint potential measurements.

The data was fitted to the unimodal van Genuchten/Mualem model (van Genuchten, 1980) and to the biomodal modification to the Genuchten model (Durner, 1994) using TensioVIEW software version 1.9 build 104 and HYPROP software version 2.0 build 89. The unimodel van Genuchten equation uses the Mualem model for conductivity (van Genuchten, 1980) and is presented in Equation 1:

$$\frac{\theta - \theta_r}{\theta_s - \theta_r} = \frac{1}{[1 + (\alpha|h|)^n]^{(1-1/n)}} \quad (1)$$

where θ is the volumetric water content, h is the soil water tension or “height”, and θ_s, θ_r, α and n are model parameters. Information regarding the tensiometer

measurement theory and data fitting method are available in (Abel, et al., 2013, Peters, et al., 2011, Schindler, et al., 2010) and from the manufacturer. Plant available water capacity was calculated as the difference in volumetric water content between FC at pF = 2.53 and PWP at pF = 4.19 using the fitted models.

5.4 Results and Implications

Mean values of soil quality indicator measurements are presented in Tables 5.1 and 5.2. The results were analyzed separately according to soil textures to evaluate the impacts of biochar from different feedstocks on soil quality indicators.

5.4.1 Coarse Textured Soil (Sandy Loam)

While pH did not show a significant difference with biochar treatment (Table 5.1), the trends of the biochar treatment impact on soil EC, SOM, Na, Ca, and Mg were similar across the coarse textured soil samples. CGT led to significantly higher EC, SOM, Na, Ca, and Mg compared to the control treatment and the other biochar treatments (Table 5.2). The EC increase in the soil amended with CGT (7.12 dS m^{-1}) is of a great concern and implies that biochar produced from CGT may lead to high salinity. Since salinity management is very critical to the success of the cropping systems in the desert southwest region, it is important to avoid the addition of materials that will exacerbate salinity problems. Although the SOM was significantly increased by the CGT in sandy soil, the corresponding increase in salinity may limit the use of CGT biochar. SAR gave significant differences in the sandy soil, but these values were well below the SAR level at which sodicity becomes a problem (SAR >13).

While NO_3-N was not significantly affected by different biochars, both P and K were significantly increased by the biochar from CGT (Table 5.2). Amending sandy soil with CGT biochar led to a P increase of about 4.2 times and a K increase of about 13.9 times compared with the control treatment. These increases are considerable in terms of nutrient additions to the soil. For micronutrients, Cu was not significantly affected by the biochar treatments, but Mn was significantly increased by the biochar treatments relative to the control (Table 5.2). There were statistical significant differences in Fe for the coarse textured soil, however, these differences do not have crop management significance since all the Fe values measured were in the medium range based on soil nutrient sufficiency levels for arid soils (Flynn, 2012). Addition of CGT and PP biochars led to significantly higher Zn levels in soil compared to the control, PS, and YW treatments. Based on crop sufficiency level, the Zn level moved to the high range with the addition of CGT and PP biochars, while it stayed in the medium range for the control, PS and YW biochar treatments (Flynn, 2012).

Table 5.1. Soil quality measurements of biochar-amended soils including pH, electrical conductivity (EC), soil organic matter (SOM), cations (Na, Ca, Mg), and calculated sodium adsorption ratio (SAR). PS: pecan shell; PP: pecan prunings; YW: yard waste; CGT: cotton gin trash.

Soil	Biochar Treatment	pH	EC (dS m^{-1})	SOM (g kg^{-1})	Na (mg kg^{-1})	Ca (mg kg^{-1})	Mg (mg kg^{-1})	SAR
Sandy loam	Control	7.45	1.45 a	0.55 a	8.3 a	5.0 a	1.4 a	4.5 b
	PS	7.48	1.28 a	0.49 a	6.6 a	4.9 a	1.2 a	3.7 ab
	PP	7.40	2.00 a	0.51 a	9.5 a	8.8 a	2.6 a	3.9 ab
	CGT	7.41	7.12 b	1.16 b	17.0 b	49.6 b	16.3 b	2.9 a
	YW	7.43	1.25 a	0.65 a	6.7 a	4.8 a	1.4 a	3.8 ab
		ns						
Clay loam	Control	6.90 a	6.86 a	1.19 a	23.5 a	47.2 a	13.8 a	4.3 a
	PS	7.03 ab	7.47 a	1.20 a	28.4 a	52.0 a	15.4 a	4.9 ab
	PP	6.88 a	15.5 c	1.24 a	62.9 c	133 c	35.3 b	6.9 c
	CGT	7.08 b	9.12 ab	1.89 b	35.2 ab	64.5 ab	23.0 a	5.3 b
	YW	6.90 a	12.0 b	1.33 a	44.5 b	94.9 b	24.7 a	5.7 b

Data are separated by soil type; entries in the same column labeled with different letters had statistically significant differences ($P < 0.05$, $n = 4$); ns: not significant at $P < 0.05$.

Table 5.2. Extractable macronutrients (NO_3-N, P, K) and micronutrients (Cu, Mn, Fe, Zn) of biochar-amended soils. PS: pecan shell; PP: pecan prunings; YW: yard waste; CGT: cotton gin trash.

Soil	Biochar Treatment	NO_3-N	P	K	Cu	Mn	Fe	Zn
		(mg kg^{-1})						
Sandy loam	Control	3.7	6.0 a	26 a	1.2	3.4 a	2.7 b	0.86 a
	PS	2.5	6.1 a	34 a	1.1	6.1 b	2.8 b	0.88 a
	PP	2.7	7.1 a	43 a	1.0	8.4 c	2.6 ab	1.12 b
	CGT	0.8	25 b	361 b	0.9	11.6 d	2.4 a	1.08 b
	YW	1.9	6.4 a	35 a	1.2	8.7 c	2.5 ab	0.90 a
		ns			ns			
Clay loam	Control	136 a	12 a	60 a	2.3	4.5 a	3.4 b	0.88
	PS	138 a	13 a	70 a	1.6	7.0 b	3.6 b	0.95
	PP	759 c	12 a	113 c	2.1	7.5 bc	2.5 a	1.19
	CGT	1 a	28 b	252 d	1.7	8.2 cd	2.8 a	1.07
	YW	466 b	13 a	92 b	1.5	8.8 d	2.7 a	1.94
					ns			ns

Data are separated by soil type; entries in the same column labeled with different letters had statistically significant differences ($P < 0.05$, $n = 4$); ns: not significant at $P < 0.05$.

5.4.2 Fine Textured Soil (Clay Loam Soil)

In the fine textured soil, the CGT led to slightly higher pH (7.08) compared to the

control treatment (pH = 6.90, see Table 5.1). This slight rise in pH was statistically significant yet would not have much management significance since nutrient availability, which is governed by soil pH, would be similar within the range of pH differences measured in this experiment. EC in the fine textured soil was highest with PP biochar amendment (15.5 dS m^{-1}) followed by YW biochar (12.0 dS m^{-1}) and CGT biochar (9.12 dS m^{-1}); these high EC levels show the need for caution in using these biochars in clay soils. As previously discussed, high EC can limit crop productivity and act as a yield constraint. Similar to the sandy soil results, CGT led to a significant increase in SOM. Na, Ca, and Mg concentrations were also affected by biochar treatments, with PP biochar-amended soils having the highest concentrations of these elements.

The NO_3-N levels were generally very high in the fine textured soil relative to the coarse textured soil, except for the CGT treatment, which was very low (Table 5.2). NO_3-N was significantly highest under the PP biochar treatment followed by YW. The reason for the very low level of NO_3-N for CGT treatment in fine textured soil is not clear, however, similar observation was made in the coarse textured soil in which the NO_3-N was quantitatively the lowest, though not significantly different. One possible explanation is that the CGT contained sufficient quantity of labile carbon such that soil microbial consumption of the labile carbon led to immobilization of plant-available nitrogen (Deenik, et al., 2010); this possibility is supported by the observation of some dark brown rather than black components of the CGT biochar.

Similar to the coarse textured soil, the CGT treatment had the highest P and K levels (Table 5.2) suggesting the possibility of nutrient additions to the soil through biochar produced from CGT. For micronutrients in the fine textured soil, Cu and Zn did not give any significant treatment effects, while Mn was highest in YW biochar treatment and Fe was highest in PS treatment. Such increases in Fe and Mn may not have significant crop management effects, however, since the measurements for all treatments belong to the same crop management ranges (medium for Fe and high for Mn (Flynn, 2012)).

5.4.3 Soil Quality Implications of This Study

This study has demonstrated the potential of biochar from different feedstocks for soil amendment. While different biochars have shown the potential to add nutrients such as nitrate, phosphate and potassium to the soil, care has to be taken with respect to the potential of each biochar to cause soil salinity. Also, the reaction of the soil to biochar produced from different feedstocks varies with soil texture. The CGT biochar, with its higher mineral content, exhibits a great potential to add organic matter to the soil and high quantities of nutrients such as P and K in both fine and coarse textured soil (Brewer, et al., 2011); however, for arid soils, the high level of salinity encountered in the CGT biochar-amended soil may serve as critical limitation to the use of this biomass feedstock. In the coarse textured soil, other biochars apart from CGT did not appear to deliver much nutrient benefits to the soil, however, they did not raise the salinity of the soil significantly when compared to the control treatment, indicating that they might

be used for long term building of the soil organic matter and soil quality. In the fine textured soil, though the control soil had initially high salinity, all the biochars tend to lead to increased salinity, except the PS biochar. Therefore, pecan shell biochar may be the best choice among the locally available feedstocks for the clay soil when salinity is considered. In order to better understand the effects of these biochar on soil quality, especially the effects on soil salinity, biochar amendments need to be tested under real field conditions and under different cropping systems.

5.4.4 Soil Moisture Desorption Results

An example of the data and the fitted model curves is show in Figure 5.1, as well as the locations of definitions of field capacity (FC) and permanent wilting point (PWP). Unimodal and bimodal van Genuchten model parameters are tabulated for the biochar-amended soils in Tables 5.3 and 5.4, respectively, as well as the estimated soil bulk densities and calculated available water capacities (AWC).

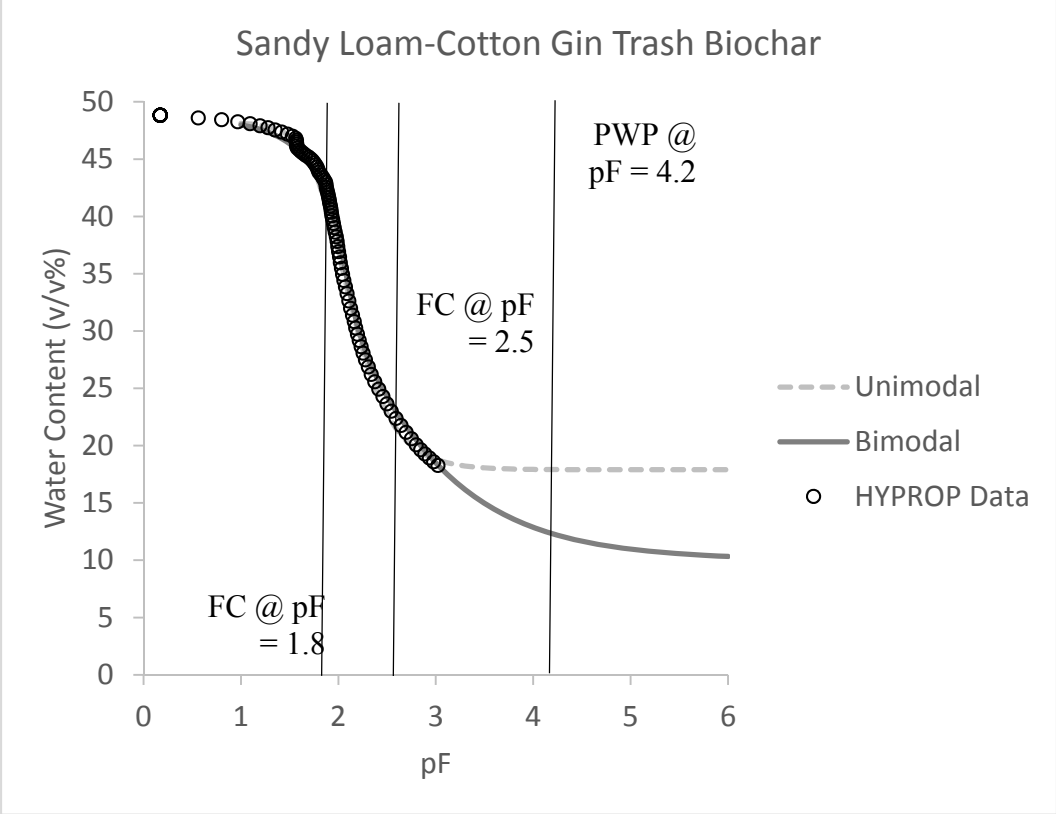

Figure 5.1 Water desorption curve data for cotton gin trash biochar-amended sandy loam soil. pF = -log(h) where h is water tension in cm of water; unimodal: water desorption curve using van Genuchten unimodal model data fit (van Genuchten, 1980); bimodal: water desorption curve using van Genuchten bimodal model data fit (Durner, 1994). Vertical lines indicate commonly-used definitions of field capacity (FC) and permanent wilting point (PWP).

Table 5.3. Soil bulk density, van Genuchten unimodal model parameters (van Genuchten, 1980), and available water content (AWC) of biochar-amended soils from water desorption measurements. AWC assumes field capacity at -33 kPa and permanent wilting point at -1.5 MPa. PS: pecan shell; PP: pecan prunings; YW: yard waste; CGT: cotton gin trash; number indicates replicate identifier from soil incubation. *Model was fit after data from dewpoint potentiometer was included.

Soil	Biochar Treatment	Bulk Density (g cm^{-3})	θ_r (cm^3 cm^{-3})	θ_s (cm^3 cm^{-3})	α (cm^{-1})	n	AWC (cm^3 cm^{-3})
Sandy Loam	Control 3	1.48	0.054	0.346	0.0116	2.474	3.8
	Control 4	1.45	0.113	0.375	0.0100	2.465	4.2
	PP 3	1.26	0.232	0.512	0.0113	2.322	4.6
	PP 3*	1.26	0.133	0.519	0.0146	1.534	13.8
	CGT 2	1.33	0.109	0.412	0.0107	2.480	4.4
	CGT 3	1.45	0.046	0.343	0.0098	2.663	3.9
	YW 3	1.40	0.081	0.392	0.0120	2.152	5.9
	YW 4	1.41	0.083	0.380	0.0104	2.399	4.9
Clay Loam	Control 3	1.22	0.051	0.447	0.0150	1.355	15.9
	PS 3	1.16	0	0.496	0.0215	1.184	16.8
	PP 2	1.17	0.176	0.548	0.0116	1.334	16.1
	PP 3	1.07	0	0.588	0.0148	1.182	21.0
	CGT 2	1.14	0	0.549	0.0137	1.216	21.1
	YW 4	1.01	0.212	0.608	0.0129	1.458	15.9

In general, the unimodal van Genuchten model was able to fit the data well near saturation but began to deviate from the tensiometer measured data as the water tensions approached PWP. This deviation would result in an underestimation of the AWC (Figure 5.1 and Table 5.3). The addition of available data from the dewpoint potentiometer for the sandy loam amended with pecan pruning biochar caused a substantial change in the fitted model parameters and increased the estimated AWC from 4.6 to 13.8 cm^3 cm^{-3}. This additional data supports the likelihood of the unimodel model underestimating the AWC.

For the sandy loam soils using the unimodal model fit, amendment with biochar did not appear to impact the AWC, except for the yard waste biochar, which showed a slight increase in AWC. More data is needed to determine if this increase is statistically significant. For the clay loam soils using the unimodal model fit, amendment with all of the biohcars except for the yard waste biochar appeared to increase the AWC, although only slightly. Again, more data would be needed to determine statistical significance.

Table 5.4. Van Genuchten bimodal model parameters (Durner, 1994) and available water content (AWC) of biochar-amended soils from water desorption measurements. AWC assumes field capacity at -33 kPa and permanent wilting point at -1.5 MPa. PS: pecan shell; PP: pecan prunings; YW: yard waste; CGT: cotton gin trash; number indicates replicate identifier from soil incubation. *Model was fit after data from dewpoint potentiometer was included.

Soil	Biochar Treatment	θ_r (cm^3 cm^{-3})	θ_s (cm^3 cm^{-3})	α_1 (cm^{-1})	n_1	α_2 (cm^{-1})	n_2	ω_2	AWC (cm^3 cm^{-3})
Sandy Loam	Control 3	0	0.350	0.0099	4.557	0.0176	1.487	0.646	7.9
	Control 4	0	0.380	0.0084	4.500	0.0198	1.260	0.669	9.8
	PP 3	0	0.517	0.0099	4.474	0.0185	1.179	0.764	13.8
	PP 3*	0.074	0.516	0.0099	4.599	0.0170	1.254	0.739	12.7
	CGT 2	0	0.384	0.0089	5.844	0.0127	1.474	0.744	11.5
	CGT 3	0	0.344	0.0094	7.018	0.0107	1.771	0.733	8.5
	YW 3	0	0.393	0.0118	3.655	0.0124	1.430	0.693	11.6
	YW 4	0	0.384	0.0090	5.841	0.0129	1.474	0.744	11.4
Clay Loam	Control 3	0	0.445	0.0211	1.936	0.0041	1.330	0.703	18.8
	PS 3	0.213	0.494	0.0269	1.493	0.0020	2.561	0.262	11.9
	PP 2	0.257	0.548	0.0129	1.468	0.0021	5.469	0.052	12.4
	PP 3	0.268	0.586	0.0209	1.498	0.0022	2.107	0.327	14.8
	CGT 2	0.211	0.547	0.0234	1.697	0.0030	1.729	0.557	16.0
	YW 4	0	0.608	0.0135	1.536	0.0003	1.895	0.425	32.1

From the bimodal model parameters, it appeared that amending sandy loam soil with pecan pruning and yard waste biochars increased the AWC by approximately 20-50%, which would be a substantial improvement if this difference were shown to be significant. Cotton gin trash biochar amendment did not appear to affect the AWC of the sandy loam soil. For the clay loam soil, amendment with biochar appeared to actually decrease AWC with the exception of yard waste biochar. As with the previous results, more data is needed to determine if these differences are consistent across replications and statistically significant. For the bimodal model, addition of the data from the dewpoint potentiometer decreased the estimated AWC slightly.

Results from previous attempts to study the impact of biochar amendment on AWC can be difficult to interpret depending on how FC and PWP are defined. For example, the FC was defined as 10 kPa (pF = 2) for a study of grass biochar added at four rates on a coarse sand soil (Jeffery, et al., 2015), while FC was defined as 6 kPa (pF = 1.8) for a study of maize silage biochar and hydrochar added to two sandy soils and four loamy sand soils (Abel, et al., 2013). As can be seen in Figure 5.1, defining FC at pF = 1.8 for the sandy loam soils here would greatly increase the absolute values of the AWC measurements and should be considered in future work. Another possibility is attempt to match the model definitions with practical measurements as was done in a study of wood mill waste gasification char study on a range of soils from loamy sand to silty clay

loam; in this case, FC was defined by the moisture content of soil that no longer wet a paper towel through drainage holes in the bottom of the pot and PWP was defined as the moisture content when wheat seedlings wilted and did not recover (Peake, et al., 2014).

5.5 Conclusions and Future Work

Amending clay loam and sandy loam agricultural soils with biochars from pecan shells, pecan orchard prunings, and yard waste had few significant impacts, positive or negative, on the soil quality indicators measured in this study after a short soil incubation. Biochar effects were different for the two different soil textures. Cotton gin trash biochar showed the greatest potential to increase soil organic matter and plant nutrients, however, the increases in salinity for both soils is a serious concern.

Biochar application rate in this trial was very high (45 Mg ha^{-1}), and the biochar materials were ground to pass through 2-mm sieve before application to the soil in order to accelerate the biochar's interactions within the soil system. It is possible that the effects seen in this trial, such as biochar's impact on soil salinity, may not be as severe if biochars are applied as larger fragments and at lower rates.

More research is needed on the effects of different biochar amendments on soil quality and plant available water retention in arid agricultural soils. Trials involving impacts of different sizes and rates of biochar are needed in arid regions, to help balance the utility of this potential soil organic matter source without delivering any negative side effect such as increased soil salinity. Work to understand the effects of biochar amendment on AWC needs to include an expanded set of instrumental data (tensiometer, dewpoint potentiometer, pressure plate) and complementary data from plant measurements. For irrigated crop systems, biochar amendments needs to be considered from both the soil water desorption and adsorption directions.

6. Outcomes of This Research

6.1 Research Capacity Building

This project served as the launching point for research laboratory and collaboration development, and several student research opportunities for one new assistant professor in Chemical & Materials Engineering (Brewer) and one assistant professor in Extension Plant Science/Plant & Environmental Science who has now been promoted to associate professor with tenure (Idowu). Funds from this project, combined with faculty start-up funds, contributed to the purchase and set up of several pieces of equipment, namely a lab-scale pyrolysis system and additional test units for soil water retention equipment. Collaborations were created or fostered between the PIs and researchers/staff at New Mexico State University in the Institute for Energy & the Environment (IEE), the Manufacturing Technology & Engineering Center, the Office of Sustainability, the Department of Building & Grounds, and the Department of Plant & Environmental Sciences, and with a research group in Chemical & Biomolecular Engineering at Rice University. Two graduate students and two undergraduate students received training in research methods, sample analysis, and laboratory safety, as well as experience in conducting original research.

6.2 Theses, Publications, and Presentations

Work on this project has resulted in one manuscript under peer review, one manuscript in revision, and two manuscripts in preparation (titles are tentative), part of one in-progress Ph.D. dissertation, part of one completed M.S. thesis, and four conference presentations:

Amiri, A., Brewer, C.E., Biomass as a renewable energy source for water desalination: a review, *in revision.*

Zhang, Y., Idowu, O.J., Brewer, C.E., Using agricultural residue biochar to improve soil quality of desert soils, *under review*.

Amiri, A., Zhang, Y., Idowu, O.J., Brewer, C.E., Design of biomass pyrolyzer-multiple effect distillation system interface, *in preparation*.

Carrillo, B.D., Yamashita, F.M., Zhang, Y., Idowu, O.J., Brewer, C.E., Biochar impacts on soil water retention of desert agricultural soils, *in preparation*.

Amiri, A., Biomass as a renewable energy source for brackish water thermal desalination, Ph.D. Dissertation, Engineering: Chemical Engineering, New Mexico State University, expected Fall 2016.

Zhang, Y., Design of biomass pyrolyzer-multiple effect distillation system components for laboratory testing, M.S. Thesis, Chemical Engineering, New Mexico State University, June 2015.

Amiri, A., Brewer, C.E., Idowu, O.J., Aspen simulation of biomass slow pyrolyzer-multiple effect distillation (MED) prototype, *1st Annual Rocky Mountain Section American Water Works Association/RMWEA Conference*, Albuquerque, NM, April 30, 2015.

Zhang, Y., Amiri, A., Brewer, C.E., Idowu, O.J., Design and testing of biomass pyrolyzer-multiple effect distillation system components for laboratory testing, *2015 American Institute of Chemical Engineers Spring Meeting*, Austin, TX, April 28, 2015.

Amiri, A., Brewer, C., Zygourakis, K., A partial-combustion model for an energy + biochar reactor design, *2014 American Institute of Chemical Engineers Annual Meeting*, Atlanta, GA, November 16, 2014.

Amiri, A., Brewer, C.E., Design of a biomass slow pyrolyzer-multiple effect distillation (MED) prototype, *Symposium on Thermal and Catalytic Sciences for Biofuels and Biobased Products*, Denver, CO, September 3, 2014.

6.3 Follow-On Proposals

Research conducted during this project has resulted in the submission of two directly related follow-on proposals, the first of which was funded and recently competed, and the second of which was not funded but did progress to Phase II consideration and is currently be revised for resubmission:

“Construction of MED Component of Pyrolysis-Desalination Unit for Resiliency Testing”
NMSU Institute of Energy & the Environment Tier 1 Supplemental Extension
8/1/14-7/31/15, $104,237, PI: Brewer
Construction and testing of a lab-scale prototype of the multiple effect distillation (MED) component of a biomass pyrolysis-water desalination unit.

"Halophytes and Biochar for Desalination Concentrate Management"
US Department of Interior/Bureau of Reclamation Desalination and Water Purification Research & Development
12/1/15-12/31/16, $149,977, PIs: Brewer, Rastegary, Idowu

Collaborations fostered through this research project have resulted in the submission of three additional related proposals, the first of which was funded and is underway; the other two of which are currently pending:

“Sustainable Use of Biomass Resources in a Semi-Arid Landscape: Connecting Chemical Engineering, Soil Science, and Extension”
USDA NIFA National Needs Fellowship
7/15/15-7/14/20, $241,000, PIs: Brewer, Ulery, Idowu, Archarya, Rockstraw
A multidisciplinary graduate fellowship program with training in chemical

engineering and soil science. This program will prepare four fellows (2 MS, 2 PhD) to address the challenges of producing food, fiber, and fuel from biomass while improving soil quality in water-limited regions.

"Invasive Plant Biomass Conversion to Biochar: A Conservation Practice to Restore Ecosystem Health"
USDA Natural Resources Conservation Service Conservation Innovation Grant
10/1/15-9/30/18, $577,666, PIs: Ganguli, Bockness, Sterling, Brewer, Ulery, Conley, Brown
Collaboration with range sciences from several universities to study the use of slow pyrolysis in the field to mitigate the spread and damage from woody invasive species.

"Holistic Approach for Sustainable Agriculture"
USDA AFRI Water for Agriculture
1/1/16-12/31/19; $10,000,000, PIs: Ghassemi, et al.
Large, multi-institutional, long-term integrated research, extension and education project focusing on water desalination techniques, use of algal and halophyte biomass, algal food products, and on-farm nutrient, water and energy use.

6.4 Other Products

Other products that are the result of this project include:

- soil samples amended with biochars made from local biomass that are available for further analysis and study;
- an Aspen Plus® simulation file allowing model experimentation with different scales and conditions for the biomass pyrolyzer-MED interface;
- a press release and extension materials about the biochar-amended soil analysis results (in preparation); and
- a webpage describing the project and results: http://wordpress.nmsu.edu/cbrewer/projects/

Reference List

[International Desalination Association] 2012. *2011-2012 IDA Deslination Yearbook*, Global Water Intelligence, London.

[U.S. Department of Energy] 2015. *Furnaces and Boilers*, Energy Savers, U.S. Department of Energy, Washington D.C., Available at: http://energy.gov/energysaver/articles/furnaces-and-boilers [Accessed 28 August 2015].

Abel, S., A. Peters, S. Trinks, H. Schonsky, M. Facklam and G. Wessolek, 2013. Impact of biochar and hydrochar addition on water retention and water repellency of sandy soil, *Geoderma*, 202–203, 183-191.

Ackermann, T. and L. Söder, 2002. An overview of wind energy-status 2002, *Renew. Sust. Energ. Rev.*, 6, 67-127.

Akash, B.A. and M.S. Mohsen, 1998. Potentials for development of hydro-powered water desalination in Jordan, *Renew. Energ.*, 13, 537-542.

Al-Anezi, K. and N. Hilal, 2007. Scale formation in desalination plants: effect of carbon dioxide solubility, *Desalination*, 204, 385-402.

Al-Jaroudi, S.S., A. Ul-Hamid and J.A. Al-Matar, 2010. Prevention of failure in a distillation unit exhibiting extensive scale formation, *Desalination*, 260, 119-128.

Al-Karaghouli, A. and L.L. Kazmerski, 2013. Energy consumption and water production cost of conventional and renewable-energy-powered desalination processes *Renew. Sust. Energ. Rev.*, 24, 343-356.

Al-Karaghouli, A., D. Renne and L.L. Kazmerski, 2009. Solar and wind opportunities for water desalination in the Arab regions, *Renew. Sust. Energ. Rev.*, 13, 2397-2407.

Al-Rawajfeh, A.E., 2010. $CaCO_3$-CO_2-H_2O system in falling film on a bank of horizontal tubes: model verification, *J. Ind. Eng. Chem.*, 16, 1050-1058.

Al-Rawajfeh, A.E., H. Glade, H.M. Qiblawey and J. Ulrich, 2004. Simulation of CO_2 release in multiple-effect distillers, *Desalination*, 166, 41-52.

Al-Shammiri, M. and M. Safar, 1999. Multi-effect distillation plants: state of the art, *Desalination*, 126, 45-59.

Annamalai, K., J.M. Sweeten and S.C. Ramalingam, 1987. Estimation of gross heating values of biomass fuels, *Transactions of the ASAE*, 30, 1205-1208.

Awerbuch, L., T.E. Lindemuth, S.C. May and A.N. Rogers, 1976. Geothermal energy recovery process, *Desalination*, 19, 325-336.

Babu, B.V., 2008. Biomass pyrolysis: a state-of-the-art review, *Biofuels, Bioproducts and Biorefining*, 2, 393-414.

Barbier, E., 2002. Geothermal energy technology and current status: an overview, *Renew. Sust. Energ. Rev.*, 6, 3-65.

Barrow, C.J., 2012. Biochar: potential for countering land degradation and for improving agriculture, *Appl. Geogr.*, 34, 21-28.

Bourouni, K., M.T. Chaibi and L. Tadrist, 2001. Water desalination by humidification and dehumidification of air: State of the art, *Desalination*, 137, 167-176.

Bourouni, K., J.C. Deronzier and L. Tadrist, 1999. Experimentation and modelling of an innovative geothermal desalination unit, *Desalination*, 125, 147-153.

Bourouni, K., R. Martin and L. Tadrist, 1999. Analysis of heat transfer and evaporation in geothermal desalination units, *Desalination*, 122, 301-313.

Branca, C. and C. DiBlasi, 2003. Global kinetics of wood char devolatilization and combustion, *Energy Fuels*, 17, 1609-1615.

Braun, G., W. Hater, C.z. Kolk, C. Dupoiron, T. Harrer and T. Götz, 2010. Investigations of silica scaling on reverse osmosis membranes, *Desalination*, 250, 982-984.

Brewer, C., R. Unger, K. Schmidt-Rohr and R. Brown, 2011. Criteria to select biochars for field studies based on biochar chemical properties, *Bioenergy Res.*, 4, 312-323.

Brewer, C.E. and R.C. Brown, 2012. Biochar, Sayigh, A., *Comprehensive Renewable Energy*, Elsevier, Oxford.

Brewer, C.E., Y.-Y. Hu, K. Schmidt-Rohr, T.E. Loynachan, D.A. Laird and R.C. Brown, 2012. Extent of pyrolysis impacts on fast pyrolysis biochar properties, *J. Environ. Qual.*, 41, 1115-1122.

Brewer, C.E., K. Schmidt-Rohr, J.A. Satrio and R.C. Brown, 2009. Characterization of biochar from fast pyrolysis and gasification systems, *Environ. Prog. Sustain. Energy*, 28, 386-396.

Bridgwater, A.V., D. Meier and D. Radlein, 1999. An overview of fast pyrolysis

of biomass, *Organic Geochemistry*, 30, 1479-1493.

Brown, A.L., P.D. Brady, C.D. Mowry and T.T. Borek, 2011. *An Economic Analysis of Mobile Pyrolysis for Northern New Mexico Forests*, Report No. Albuquerque

Brown, R.C. and T.R. Brown, 2014. *Biorenwable Resources: Engineering New Products from Agriculture*, Wiley-Blackwell, Danvers, MA.

Brown, T.R., M.M. Wright and R.C. Brown, 2011. Estimating profitability of two biochar production scenarios: slow pyrolysis vs fast pyrolysis, *Biofuel. Bioprod. Bior.*, 5, 54-68.

Cardona, E., S. Culotta and A. Piacentino, 2003. Energy saving with MSF-RO series desalination plants, *Desalination*, 153, 167-171.

Channiwala, S.A. and P.P. Parikh, 2002. A unified correlation for estimating HHV of solid, liquid and gaseous fuels, *Fuel*, 81, 1051-1063.

Chen, G., J. Andries, Z. Luo and H. Spliethoff, 2003. Biomass pyrolysis/gasification for product gas production: the overall investigation of parametric effects, *Energy Conversion and Management*, 44, 1875-1884.

Cheng, C.-H., J. Lehmann and M.H. Engelhard, 2008. Natural oxidation of black carbon in soils: Changes in molecular form and surface charge along a climosequence, *Geochim. Cosmochim. Acta*, 72, 1598-1610.

Christmann, J.B.P., L.J. Krätz and H.-J. Bart, 2010. Novel polymer film heat exchangers for seawater desalination, *Desalination and Water Treatment*, 21, 162-174.

Cihacek, L.J., 1983. *Interpreting Soil Analysis*, Report No. University, N.M.S., Las Cruces, NM.

Cordero, T., F. Marquez, J. Rodriguez-Mirasol and J.J. Rodriguez, 2001. Predicting heating values of lignocellulosics and carbonaceous materials from proximate analysis, *Fuel*, 80, 1567-1571.

Daniels, F., 1974. *Direct Use of the Sun's Energy*, Ballantine Books, New York.

Darwish, M.A. and H.K. Abdulrahim, 2008. Feed water arrangements in a multi-effect desalting system, *Desalination*, 228, 30-54.

Deenik, J.L., T. McClellan, U. Goro, M.J. Antal and S. Campbell, 2010. Charcoal volatile matter content influences plant growth and soil nitrogen transformations, *Soil Sci. Soc. Am. J.*, 74, 1259-1270.

Downie, A., P. Munroe, A. Cowie, L. Van Zwieten and D.M.S. Lau, 2012. Biochar as a Geoengineering Climate Solution: Hazard Identification and Risk Management, *Critical Reviews in Environmental Science and Technology*, 42, 225-250.

Downing, M., L.M. Eaton, R.L. Graham, M.H. Langholtz, R.D. Perlack, A.F. Turhollow Jr, B. Stokes and C.C. Brandt, 2011. *U.S. Billion-Ton Update: Biomass Supply for a Bioenergy and Bioproducts Industry*, Report No. ORNL/TM-2011/224,

Durner, W., 1994. Hydraulic conductivity estimation for soils with heterogeneous pore structure, *Water Resources Research*, 30, 221-223.

Eibling, J.A., S.G. Talbert and G.O.G. Löf, 1971. Solar stills for community use—digest of technology, *Sol. Energy*, 13, 263-276.

Elimelech, M. and W.A. Phillip, 2011. The future of seawater desalination: energy, technology, and the environment, *Science*, 333, 712-717.

Eltawil, M.A., Z. Zhengming and L. Yuan, 2009. A review of renewable energy technologies integrated with desalination systems, *Renew. Sust. Energ. Rev.*, 13, 2245-2262.

Emrich, W., 1985. *Handbook of Charcoal Making: The Traditional and Industrial Methods*, Solar Energy R&D in the European Community, Series E: Energy from Biomass, Springer, Luxembourg.

Erol, M., H. Haykiri-Acma and S. Kucukbayrak, 2010. Calorific value estimation of biomass from their proximate analyses data, *Renewable Energy*, 35, 170-173.

Fantozzi, F., S. Colantoni, P. Bartocci and U. Desideri, 2007. Rotary kiln slow pyrolysis for syngas and char production from biomas and waste--Part 1. Working envelope of the reactor, *Journal of Engineering for Gas Turbines and Power*, 129, 901-907.

Fiorenza, G., V.K. Sharma and G. Braccio, 2003. Techno-economic evaluation of a solar powered water desalination plant, *Energ. Convers. Manage.*, 44, 2217-2240.

Flynn, R., 2012. Appropriate Analyses for New Mexico Soils, Guide A-146, Report No. Las Cruces, NM.

Galal, T., A. Kalendar, A. Al-Saftawi and M. Zedan, 2010. Heat transfer performance of condenser tubes in an MSF desalination system, *Journal of Mechanical Science and Technology*, 24, 2347-2355.

Garcia-Perez, M., C. Kruger, M. Fuchs and S. Sokhansanj, 2012. Methods for Producing Biochar and Advanced Bio-fuels in Washington State (Part II: From field to pyrolysis reactor), Report No. 12-07-033,

Garcia-Perez, M., T. Lewis and C.E. Kruger, 2010. Methods for Producing Biochar and Advanced Biofuels in Washington State, Part 1: Literature Review of Pyrolysis Reactors, Report No. 11-07-017, Ecology, S.o.W.D.o., Pullman, WA.

García-Rodríguez, L. and C. Gómez-Camacho, 1999. Preliminary design and cost analysis of a solar distillation system, *Desalination*, 126, 109-114.

García-Rodríguez, L. and C. Gómez-Camacho, 2001. Perspectives of solar-assisted seawater distillation, *Desalination*, 136, 213-218.

García-Rodríguez, L., A.I. Palmero-Marrero and C. Gómez-Camacho, 1999. Application of direct steam generation into a solar parabolic trough collector to multieffect distillation, *Desalination*, 125, 139-145.

García-Rodríguez, L., A.I. Palmero-Marrero and C. Gómez-Camacho, 2002. Comparison of solar thermal technologies for applications in seawater desalination, *Desalination*, 142, 135-142.

García-Rodríguez, L., V. Romero-Ternero and C. Gómez-Camacho, 2001. Economic analysis of wind-powered desalination, *Desalination*, 137, 259-265.

Habali, S.M. and I.A. Saleh, 1994. Design of stand-alone brackish water desalination wind energy system for Jordan, *Sol. Energy*, 52, 525-532.

Hamed, O.A., 2005. Overview of hybrid desalination systems — current status and future prospects, *Desalination*, 186, 207-214.

Hanson, A., W. Zachritz, K. Stevens, L. Mimbela, R. Polka and L. Cisneros, 2004. Distillate water quality of a single-basin solar still: laboratory and field studies, *Sol. Energy*, 76, 635-645.

Helal, A.M., A.M. El-Nashar, E. Al-Katheeri and S. Al-Malek, 2003. Optimal design of hybrid RO/MSF desalination plants Part I: Modeling and algorithms, *Desalination*, 154, 43-66.

Helal, A.M., A.M. El-Nashar, E.S. Al-Katheeri and S.A. Al-Malek, 2004. Optimal design of hybrid RO/MSF desalination plants Part II: Results and discussion, *Desalination*, 160, 13-27.

Hetsroni, G. and A. Mosyak, 1994. Heat transfer and pressure drop in a plastic heat exchanger with triangular channels, *Chem. Eng. Process.*, 33, 91-100.

Houcine, I., F. Benjemaa, M.-H. Chahbani and M. Maalej, 1999. Renewable energy sources for water desalting in Tunisia, *Desalination*, 125, 123-132.

Idowu, O.J. and R. Flynn, 2013. Understanding Soil Health for Production Agriculture in New Mexico, Guide A-148, Report No. Service, C.E., Las Cruces, NM.

Idowu, O.J., M. Marsalis and R. Flynn, 2012. *Agronomic Principles to Help with Farming During Drought Periods, Guide A-147*, Report No. Service, C.E., Las Cruces, NM.

Ioannidou, O., A. Zabaniotou, E.V. Antonakou, K.M. Papazisi, A.A. Lappas and C. Athanassiou, 2009. Investigating the potential for energy, fuel, materials and chemicals production from corn residues (cobs and stalks) by non-catalytic and catalytic pyrolysis in two reactor configurations, *Renewable and Sustainable Energy Reviews*, 13, 750-762.

Isci, A. and G.N. Demirer, 2007. Biogas production potential from cotton wastes, *Renewable Energy*, 32, 750-757.

Jeffery, S., M.B.J. Meinders, C.R. Stoof, T.M. Bezemer, T.F.J. van de Voorde, L. Mommer and J.W. van Groenigen, 2015. Biochar application does not improve the soil hydrological function of a sandy soil, *Geoderma*, 251–252, 47-54.

Jeffery, S., F.G.A. Verheijen, M. van der Velde and A.C. Bastos, 2011. A quantitative review of the effects of biochar application to soils on crop productivity using meta-analysis, *Agriculture, Ecosystems & Environment*, 144, 175-187.

Jenkins, B.M., L.L. Baxter and T.R. Miles, 1998. Combustion properties of biomass, *Fuel Processing Technology*, 54, 17-46.

Jiménez, L. and F. González, 1991. Study of the physical and chemical properties of lignocellulosic residues with a view to the production of fuels, *Fuel*, 70, 947-950.

Joo, H.-J. and H.-Y. Kwak, 2013. Performance evaluation of multi-effect distiller for optimized solar thermal desalination, *Appl. Therm. Eng.*, 61, 491-499.

Kallestad, J.C., J.G. Mexal and T.W. Sammis, 2008. Mesilla Valley Pecan Orchard Pruning Residues: Biomass Estimates and Value-Added Opportunities, Research Report 764, Report No. Las Cruces, NM.

Kalogirou, S., 1997. Survey of solar desalination systems and system selection, *Energy*, 22, 69-81.

Kalogirou, S., 2014. *Solar Energy Engineering Processes and Systems*, Academic Press, Oxford.

Kalogirou, S.A., 2005. Seawater desalination using renewable energy sources, *Prog. Energ. Combust.*, 31, 242-281.

Karagiannis, I.C. and P.G. Soldatos, 2008. Water desalination cost literature review and assesment, *Desalination*, 223, 448-456.

Karhu, K., T. Mattila, I. Bergström and K. Regina, 2011. Biochar addition to agricultural soil increased CH_4 uptake and water holding capacity – Results from a short-term pilot field study, *Agr. Ecosyst. Environ.*, 140, 309-313.

Karlen, D.L., M.J. Mausbach, J.W. Doran, R.G. Cline, R.F. Harris and G.E. Schuman, 1997. Soil quality: a concept, definition, and framework for evaluation (a guest editorial), *Soil Sci Soc Am J*, 61, 4-10.

Kim, K.H., X. Bai, M.R. Rover and R.C. Brown, 2014. The effect of low-concentration oxygen in sweep gas during pryolysis of red oak using a fluidized bed reactor, *Fuel*, 124, 49-56.

Kimetu, J., J. Lehmann, S. Ngoze, D. Mugendi, J. Kinyangi, S. Riha, L. Verchot, J. Recha and A. Pell, 2008. Reversibility of soil productivity decline with organic matter of differing quality along a degradation gradient, *Ecosystems*, 11, 726-739.

Kinney, T.J., C.A. Masiello, B. Dugan, W.C. Hockaday, M.R. Dean, K. Zygourakis and R.T. Barnes, 2012. Hydrologic properties of biochars produced at different temperatures, *Biomass Bioenerg.*, 41, 34-43.

Kiranoudis, C.T., N.G. Voros and Z.B. Maroulis, 1997. Wind energy exploitation for reverse osmosis desalination plants, *Desalination*, 109, 195-209.

Laird, D.A., 2008. The charcoal vision: A win-win-win scenario for simultaneously producing bioenergy, permanently sequestering carbon, while improving soil and water quality, *Agron. J.*, 100, 178-181.

Laird, D.A., P. Fleming, D.D. Davis, R. Horton, B. Wang and D.L. Karlen, 2010. Impact of biochar amendments on the quality of a typical Midwestern agricultural soil, *Geoderma*, 158, 443-449.

Lal, R., 2008. Black and buried carbons' impact on soil quality and ecosystem services, *Soil Till. Res.*, 99, 1-3.

Lee, J.W., M. Kidder, B.R. Evans, S. Paik, A.C. Buchanan, C.T. Garten and R.C. Brown, 2010. Characterization of biochars produced from cornstovers for soil

amendment, *Environ. Sci. Technol.*, 44, 7970-7974.

Lee, Y., P.-R.-B. Eum, C. Ryu, Y.-K. Park, J.-H. Jung and S. Hyun, 2013. Characteristics of biochar produced from slow pyorlysis of Geodae-Uksae 1, *Bioresource Technology*, 130, 345-350.

Lehmann, J. and S. Joseph, 2009. Biochar for Environmental Management: Science and Technology, Earthscan, London.

Lehmann, J., J. Pereira da Silva, C. Steiner, T. Nehls, W. Zech and B. Glaser, 2003. Nutrient availability and leaching in an archaeological Anthrosol and a Ferralsol of the Central Amazon basin: fertilizer, manure and charcoal amendments, *Plant Soil*, 249, 343-357.

Lehmann, J., M.C. Rillig, J. Thies, C.A. Masiello, W.C. Hockaday and D. Crowley, 2011. Biochar effects on soil biota - A review, *Soil Biol. Biochem.*, 43, 1812-1836.

Lenzen, M. and J. Munksgaard, 2002. Energy and CO_2 life-cycle analyses of wind turbines—review and applications, *Renew. Energ.*, 26, 339-362.

Li, D., W.C. Hockaday, C.A. Masiello and P.J.J. Alvarez, 2011. Earthworm avoidance of biochar can be mitigated by wetting, *Soil Biol. Biochem.*, 43, 1732-1737.

Li, Y.D. and H. Liu, 2000. High-pressure densification of wood residues to form an upgraded fuel, *Biomass & Bioenergy*, 19, 177-186.

Liang, B., J. Lehmann, D. Solomon, J. Kinyangi, J. Grossman, B. O'Neill, J.O. Skjemstad, J. Thies, F.J. Luizao, J. Petersen and E.G. Neves, 2006. Black carbon increases cation exchange capacity in soils, *Soil Sci. Soc. Am. J.*, 70, 1719-1730.

Likhachev, D.S. and F.-C. Li, 2013. Large-scale water desalination methods: a review and new perspectives, *Desalination and Water Treatment*, 51, 2836-2849.

Lillywhite, J.M., R. Heerema, J.E. Simonsen and E. Herrera, 2010. *Pecan Marketing Channels in New Mexico, 2010, Guide Z-307*, Report No. Las Cruces, NM.

Ludwick, A.E. and J.O. Reuess, 1974. *Guide to fertilizer recommendations in Colorado*, Report No. University, C.S., Fort Collins, CO.

Ma, Q. and H. Lu, 2011. Wind energy technologies integrated with desalination systems: Review and state-of-the-art, *Desalination*, 277, 274-280.

Magdoff, F., 2001. Concepts, components, and strategies of soil health in

agroecosystems, *Journal of Nematology*, 33, 169.

Manenti, F., M. Masi, G. Santucci and G. Manenti, 2013. Parametric simulation and economic assessment of a heat integrated geothermal desalination plant, *Desalination*, 317, 193-205.

Mani, S., L.G. Tabil and S. Sokhansanj, 2006. Specific energy requirement for compacting corn stover, *Bioresource Technology*, 97, 1420-1426.

Manolakos, D., G. Papadakis, D. Papantonis and S. Kyritsis, 2001. A simulation-optimisation programme for designing hybrid energy systems for supplying electricity and fresh water through desalination to remote areas: Case study: the Merssini village, Donoussa island, Aegean Sea, Greece, *Energy*, 26, 679-704.

Matsuoka, K., K. Kuramoto, T. Murakami and Y. Suzuki, 2008. Steam Gasification of Woody Biomass in a Circulating Dual Bubbling Fluidized Bed System, *Energy Fuels*, 22, 1980-1985.

McHenry, M.P., 2009. Agricultural bio-char production, renewable energy generation and farm carbon sequestration in Western Australia: Certainty, uncertainty and risk, *Agriculture, Ecosystems & Environment*, 129, 1-7.

Methnani, M., 2007. Influence of fuel costs on seawater desalination options, *Desalination*, 205, 332-339.

Mexal, J.G., E. Herrera, T.W. Sammis and W.H. Zachritz, 2003. *Noncommensurable Values of the Pecan Industry, Guide H-654*, Report No. Las Cruces, NM.

Miller, J.E., 2003. Review of Water Resources and Desalination Technologies, SAND 2003-0800, Report No. Laboratories, S.N., Albuquerque, NM.

Miranda, M.S. and D. Infield, 2003. A wind-powered seawater reverse-osmosis system without batteries, *Desalination*, 153, 9-16.

Munoz-Guerra, J.A., P. Prado and S.V. Garcia-Tenorio, 2011. Use of hydrogen as a carrier gas for the analysis of steroids with anabolic activity by gas chromatography/mass spectrometry, *Journal of Chromatography A*, 1218, 7365-7370.

Murakami, M., 1994. Hydro-powered reverse osmosis (RO) desalination for co-generation: A Middle East case study, *Desalination*, 97, 301-311.

Naik, S.N., V.V. Goud, P.K. Rout and A.K. Dalai, 2010. Production of first and second generation biofuels: A comprehensive review, *Renewable & Sustainable Energy Reviews*, 14, 578-597.

Ndiema, C.K.W., P.N. Manga and C.R. Ruttoh, 2002. Influence of die pressure on relaxation characteristics of briquetted biomass, *Energy Conversion and Management*, 43, 2157-2161.

Nelson, D.W. and L.E. Sommers, 1996. Total carbon, organic carbon and organic matter, Sparks, D.L., *Methods of Soil Analysis Part 3. Chemical Methods*, SSSA and ASA, Madison, WI.

Nisan, S. and N. Benzarti, 2008. A comprehensive economic evaluation of integrated desalination systems using fossil fuelled and nuclear energies and including their environmental costs, *Desalination*, 229, 125-146.

Olsen, S.R., C.V. Cole, F.S. Watanabe and L.A. Dean, 1954. Estimation of available phosphorus in soils by extraction with sodium bicarbonate, *U.S. Dept. of Agric. Circ.*, 939,

Ophir, A., 1982. Desalination plant using low grade geothermal heat, *Desalination*, 40, 125-132.

Ophir, A. and F. Lokiec, 2005. Advanced MED process for most economical sea water desalination, *Desalination*, 182, 187-198.

Park, J., Y. Lee, C. Ryu and Y.K. Park, 2014. Slow pyrolysis of rice straw: Analysis of products properties, carbon and energy yields, *Bioresource Technology*, 155, 63-70.

Peake, L.R., B.J. Reid and X. Tang, 2014. Quantifying the influence of biochar on the physical and hydrological properties of dissimilar soils, *Geoderma*, 235–236, 182-190.

Peters, A., W. Durner and G. Wessolek, 2011. Consistent parameter constraints for soil hydraulic functions, *Advances in Water Resources*, 34, 1352-1365.

Phan, A.N., C. Ryu, V.N. Sharifi and J. Swithenbank, 2008. Characterisation of slow pyrolysis products from segregated wastes for energy production, *Journal of Analytical and Applied Pyrolysis*, 81, 65-71.

Qiblawey, H.M. and F. Banat, 2008. Solar thermal desalination technologies, *Desalination*, 220, 633-644.

Quaak, P., H. Knoef and H. Stassen, 1999. *Energy from Biomass: A Review of Combustion and Gasification Technologies*, Report No. Bank, T.W., Washington, D.C.

Raluy, R.G., L. Serra and J. Uche, 2005. Life cycle assessment of desalination

technologies integrated with renewable energies, *Desalination*, 183, 81-93.

Reeves, D.W., 1997. The role of soil organic matter in maintaining soil quality in continuous cropping systems, *Soil and Tillage Research*, 43, 131-167.

Robinson, R., G. Ho and K. Mathew, 1992. Development of a reliable low-cost reverse osmosis desalination unit for remote communities, *Desalination*, 86, 9-26.

Sarkar, M., A. Kumar, J.S. Tumuluru, K.N. Patil and D.D. Bellmer, 2014. Gasification performance of switchgrass pretreated with torrefaction and densification, *Applied Energy*, 127, 194-201.

Schindler, U., W. Durner, G. von Unold, L. Mueller and R. Wieland, 2010. The evaporation method: Extending the measurement range of soil hydraulic properties using the air-entry pressure of the ceramic cup, *Journal of Plant Nutrition and Soil Science*, 173, 563-572.

Semiat, R., 2008. Energy issues in desalination processes, *Environ. Sci. Technol.*, 42, 8193-8201.

Semiat, R. and D. Hasson, 2012. Water desalination, *Rev. Chem. Eng.*, 28, 43-60.

Sen, P.K., P.V. Sen, A. Mudgal and S.N. Singh, 2011. A small scale multi-effect distillation (MED) unit for rural micro enterprises: Part-III Heat transfer aspects, *Desalination*, 279, 38-46.

Sen, P.K., P.V. Sen, A. Mudgal and S.N. Singh, 2011. A small scale multiple-effect distillation (MED) unit for rural micro enterprises: Part II--Parametric studies and performance analysis, *Desalination*, 279, 27-37.

Sen, P.K., P.V. Sen, A. Mudgal, S.N. Singh, S.K. Vyas and P. Davies, 2011. A small scale multiple-effect distillation (MED) unit for rural micro enterprises: Part I--design and fabrication, *Desalination*, 279, 15-26.

Sen, P.V., K. Bhuwanesh, K. Ashutosh, Z. Engineer, S. Hegde, P.K. Sen and R. Lal, 2013. Micro-scale multiple-effect distillation system for low steam inputs, *Procedia Engineering*, 56, 63-67.

Shabangu, S., D. Woolf, E.M. Fisher, L.T. Angenent and J. Lehmann, 2014. Techno-economic analysis of biomass slow pyrolysis into different biochar and methanol concepts, *Fuel*, 117, 742-748.

Shajizadeh, F. and W. Degroot, 1976. *Thermal uses and properties of carbohydrates and lignins* Academic Press, New York.

Shastri, Y.N., Z. Miao, L.F. Rodríguez, T.E. Grift, A.C. Hansen and K.C. Ting,

2014. Determining optimal size reduction and densification for biomass feedstock using the BioFeed optimization model, *Biofuels, Bioproducts and Biorefining*, 8, 423-437.

Sheng, C.D. and J.L.T. Azevedo, 2005. Estimating the higher heating value of biomass fuels from basic analysis data, *Biomass & Bioenergy*, 28, 499-507.

Skoulou, V., G. Koufodimos, Z. Samaras and A. Zabaniotou, 2008. Low temperature gasification of olive kernels in a 5-kW fluidized bed reactor for H2-rich producer gas, *International Journal of Hydrogen Energy*, 33, 6515-6524.

Smith, J.M., H.C. Van Ness and M.M. Abbott, 2005. *Introduction to Chemical Engineering Thermodynamics*, McGraw Hill Higher Education, Columbus, OH.

Staff, S.S., 1999. *Soil Taxonomy: A Basic System of Soil Classification for Making and Interpreting Soil Surveys*, U.S. Department of Agriculture Handbook 436, Natural Resources Conservation Service,

Steinbeiss, S., G. Gleixner and M. Antonietti, 2009. Effect of biochar amendment on soil carbon balance and soil microbial activity, *Soil Biol. Biochem.*, 41, 1301-1310.

Steiner, C., B. Glaser, W.G. Teixeira, J. Lehmann, W. Blum and W. Zech, 2008. Nitrogen retention and plant uptake on a highly weathered central Amazonian Ferralsol amended with compost and charcoal, *J. Plant Nutr. Soil Sci.*, 171, 893-899.

Steiner, C., W. Teixeira, J. Lehmann, T. Nehls, J. de Macêdo, W. Blum and W. Zech, 2007. Long term effects of manure, charcoal and mineral fertilization on crop production and fertility on a highly weathered Central Amazonian upland soil, *Plant Soil*, 291, 275-290.

Thoreson, C., K. Webster, M. Darr and E. Kapler, 2014. Investigation of process variables in the densification of corn stover briquettes, *Energies*, 7, 4019-4032.

Thu, K., Y.-D. Kim, G. Amy, W.G. Chun and K.C. Ng, 2013. A hybrid multi-effect distillation and adsorption cycle, *Appl. Energ.*, 104, 810-821.

Tian, L., J. Guo, Y. Tang and L. Cao, 2005. A historical opportunity: economic competitiveness of seawater desalination project between nuclear and fossil fuel while the world oil price over $50 per boe—part A: MSF, *Desalination*, 183, 317-325.

Tillman, D., 1978. *Wood as an energy resouce* Academic Press, New York

Tumuluru, J.S., C.T. Wright, J.R. Hess and K.L. Kenney, 2011. A review of

biomass densification systems to develop uniform feedstock commodities for bioenergy application, *Biofuels, Bioproducts and Biorefining*, 5, 683-707.

Tzen, E. and R. Morris, 2003. Renewable energy sources for desalination, *Sol. Energy*, 75, 375-379.

Tzen, E., K. Perrakis and P. Baltas, 1998. Design of a stand alone PV - desalination system for rural areas, *Desalination*, 119, 327-333.

Uche, J., L. Serra and A. Valero, 2001. Thermoeconomic optimization of a dual-purpose power and desalination plant, *Desalination*, 136, 147-158.

Ulery, A.L. and A.J. Tugel, 1999. Farming in New Mexico: Soil quality and productivity maintenance, *New Mexico Journal of Science*, 39, 86-108.

van Genuchten, M.T., 1980. A closed form of the equation for predicting the hydraulic conductivity of unsaturated soils, *Soil Sci Soc Am J*, 44, 892-898.

Wijayantia, W. and K.-i. Tanoue, 2013. Char formation and gas products of woody biomass pyrolysis, *Energy Procedia* 32, 145-152.

Winsley, P., 2007. Bioenergy and biochar production for climate change mitigation, *N. Z. Sci. Rev.*, 64, 5-10.

Wright, M. and R.C. Brown, 2007. Establishing the optimal sizes of different kinds of biorefineries, *Biofuels, Bioproducts and Biorefining*, 1, 191-200.

Yan, X., B. Li, B. Liu, J. Zhao, Y. Wang and H. Li, 2014. Analysis of improved novel hollow fiber heat exchanger, *Appl. Therm. Eng.*, 67, 114-121.

Yang, H., R. Yan, H. Chen, D.H. Lee and C. Zheng, 2007. Characteristics of hemicellulose, cellulose and lignin pyrolysis, *Fuel*, 86, 1781-1788.

Yang, L., S. Shen and H. Hu, 2011. Thermodynamic performance of a low temperature multi-effect distillation experimental unit with horizontal-tube falling film evaporation, *Desalination and Water Treatment*, 33, 202-208.

Yousuf, A., 2012. Biodiesel from lignocellulosic biomass - Prospects and challenges, *Waste Management*, 32, 2061-2067.

Zaheed, L. and R.J.J. Jachuck, 2004. Review of polymer compact heat exchangers, with special emphasis on a polymer film unit, *Appl. Therm. Eng.*, 24, 2323-2358.

Zanzi, R., K. Sjöström and E. Björnbom, 2002. Rapid pyrolysis of agricultural residues at high temperature, *Biomass and Bioenergy*, 23, 357-366.

Zhao, D., J. Xue, S. Li, H. Sun and Q.-d. Zhang, 2011. Theoretical analyses of thermal and economical aspects of multi-effect distillation desalination dealing with high-salinity wastewater, *Desalination*, 273, 292-298.

Appendix: Data Record

Table A.1 Yields of biochar and bio-oil from lab scale slow pyrolysis

Material	Feedstock (g)	Biochar (g)	Yield of biochar (%)	Collected bio-oil (g)	Yield of bio-oil (%)
Pecan Shell	242.1	66.8	27.6	44	18
Pecan Prunings	250.7	87.7	35.0	33	13
Yard Waste	195.0	61.5	31.5	33	17
Cotton Gin Trash	252.3	106.1	42.1	28	11

Table A.2 Moisture content of biochars and feedstocks

Product	Sample + holder (g)	Wet sample (g)	Dry sample (g)	Moisture (%)
Pecan Shell	6.04	5.17	5.83	3.9
Pecan Prunings	2.87	1.95	2.79	4.3
Yard Waste	2.23	1.27	2.20	2.4
Cotton Gin Trash	3.49	2.83	3.39	3.3
Feedstock				
Pecan Shell	24.26	22.04	22.99	5.8
Pecan Prunings	23.47	21.02	22.27	5.7
Yard Waste	25.91	23.92	24.91	4.2
Cotton Gin Trash	14.60	12.92	13.81	6.1

Table A.3 Ash contents of biochars and feedstocks.

Products	Rep.	Crucible (g)	Sample + crucible (g)	Ash + crucible (g)	Ash content (%)
Pecan Shell	1	12.41	13.41	12.45	4.19
	2	12.43	13.37	12.47	4.27
Pecan Prunings	1	11.85	12.55	11.93	10.90
	2	13.32	14.34	13.43	10.62
Yard Waste	1	12.02	12.47	12.09	16.96
	2	17.79	18.41	17.92	21.90
Cotton Gin Trash	1	12.93	13.70	13.14	27.58
	2	18.06	19.31	18.49	34.54
Feedstock					
Pecan Shell	1	16.02	16.59	16.03	1.74
	2	17.19	17.74	17.19	1.08
Pecan Prunings	1	28.29	28.85	28.31	2.52
	2	15.55	16.03	15.56	2.87
Cotton Gin Trash	1	28.29	28.84	28.36	11.40
	2	15.55	16.05	15.61	13.41
Yard Waste	1	16.02	16.56	16.04	4.39
	2	17.19	17.69	17.21	5.02

Table A.4 Higher heating values (HHV) of biochars and feedstocks, measured by bomb calorimetry.

Sample	HHV (MJ/kg)	
Feedstocks		
Pecan shell	18.6	17.9
Cotton gin trash	17.6	16.0
Yard Waste	23.5	20.2
Pecan prunings	20.5	24.6
Biochars		
Pecan shell	31.7	29.7
Cotton gin trash	21.7	26.0
Pecan prunings	32.6	29.4
Yard waste	28.5	34.4

Table A.5 Analysis results for biochar-amended sandy loam soils after incubation. EC: electrical conductivity; SAR: sodium adsorption ratio; OM: organic matter.

BiocharTrt	Block	pH	EC	Mg	Ca	Na	SAR	OM	Nitrate-N	K	P	Zn	Mn	Fe	Cu	% Saturation
			dS/m	mg/kg				g/kg	mg/kg							
Control	1	7.40	0.582	0.46	1.87	3.16	2.93	0.53	1.05	23.4	6.21	0.85	3.28	2.89	1.38	27.04
Control	2	7.50	1.52	1.4	4.83	8.03	4.55	0.47	1.47	25.0	5.88	0.85	3.28	2.64	1.33	19.95
Control	3	7.40	2.26	2.61	8.58	14.25	6.02	0.53	10.8	28.3	5.69	0.87	4.17	2.56	1.08	21.97
Control	4	7.50	1.42	1.15	4.58	7.72	4.56	0.66	1.44	26.0	6.08	0.85	3.03	2.78	1.20	22.15
YardWaste	1	7.40	0.614	0.56	2.08	3.6	3.13	0.58	0.65	33.0	6.34	0.82	7.56	2.39	1.14	29.17
YardWaste	2	7.30	1.14	1.8	5.5	5.0	2.62	0.71	0.24	29.4	6.21	1.0	8.69	2.58	1.85	25.34
YardWaste	3	7.50	1.58	1.49	5.48	7.98	4.27	0.59	2.91	37.4	6.21	0.87	9.14	2.52	1.0	26.58
YardWaste	4	7.50	1.68	1.72	6.05	10.2	5.17	0.72	3.72	40.8	6.73	0.91	9.3	2.61	0.99	28.37
PecanSh	1	7.53	0.786	0.85	3.45	3.31	2.26	0.47	1.91	29.1	6.47	0.86	5.46	2.81	1.09	24.89
PecanSh	2	7.50	1.22	1.15	4.54	6.19	3.67	0.52	5.87	34.6	6.08	0.9	5.59	2.85	1.2	31.50
PecanSh	3	7.50	1.43	1.25	5.09	7.58	4.26	0.51	0.70	36.4	5.95	0.86	6.47	2.73	1.07	25.93
PecanSh	4	7.40	1.67	1.68	6.35	9.14	4.56	0.44	1.57	36.8	5.95	0.91	6.73	2.7	1.07	26.46

Table A.5, continued.

BiocharTrt	Block	pH	EC	Mg	Ca	Na	SAR	OM	Nitrate-N	K	P	Zn	Mn	Fe	Cu	% Saturation
			dS/m	mg/kg				g/kg	mg/kg							
CotTrash	1	7.32	4.41	8.28	24.8	9.48	2.33	1.42	0.70	204.0	23.3	1.02	10.0	2.68	1.03	27.81
CotTrash	2	7.42	8.08	18.6	53.2	18.6	3.10	0.93	1.05	476.0	25.97	1.05	12.71	2.14	0.85	32.15
CotTrash	3	7.40	8.11	18.6	55.9	19.4	3.18	1.18	0.73	379.0	24.53	1.08	11.65	2.27	0.74	26.90
CotTrash	4	7.50	7.86	19.7	64.4	20.5	3.16	1.11	0.71	386.0	25.61	1.15	11.96	2.35	1.08	28.43
PecanTree	1	7.50	0.837	0.89	3.73	3.51	2.31	0.47	1.18	32.5	8.33	1.05	7.57	2.52	0.78	28.07
PecanTree	2	7.40	2.44	3.18	10.4	11.5	4.41	0.62	1.66	48.4	7.13	1.12	8.95	2.58	1.05	29.48
PecanTree	3	7.40	2.24	2.8	9.46	11.3	4.56	0.45	1.21	42.0	6.34	1.11	8.37	2.73	1.14	26.83
PecanTree	4	7.30	2.47	3.38	11.8	11.5	4.17	0.49	6.94	48.4	6.6	1.2	8.61	2.61	1.02	26.85

Table A.6 Analysis results for biochar-amended clay loam soils after incubation. EC: electrical conductivity; SAR: sodium adsorption ratio; OM: organic matter.

BiocharTrt	Block	pH	EC	Mg	Ca	Na	SAR	OM	Nitrate-N	K	P	Zn	Mn	Fe	Cu	% Saturation
			dS/m	mg/kg				g/kg	mg/kg							
Control	1	6.90	6.02	12.6	41.8	20.9	4.01	1.31	128.9	63.4	11.09	0.86	5.42	3.35	1.99	41.93
Control	2	6.90	6.86	13.8	45.2	25.1	4.62	1.17	92.2	55.6	11.8	0.87	4.26	3.50	1.49	44.90
Control	3	6.90	6.18	12.1	42.3	21.6	4.14	1.15	109.3	58.2	12.52	0.74	3.82	3.42	1.44	51.79
Control	4	6.90	8.36	16.8	59.3	26.2	4.25	1.11	215.4	63.9	13.4	1.05	4.55	3.26	4.35	45.82
YardWaste	1	7.00	8.61	17.0	59.7	29.8	4.81	1.26	283.9	82.8	12.09	5.36	8.03	3.06	1.43	54.05
YardWaste	2	6.80	10.8	24.6	85.9	43.9	5.91	1.32	345.6	89.1	12.67	0.78	7.67	2.77	1.32	43.11
YardWaste	3	6.88	14.4	30.7	114.0	59.1	6.95	1.47	585.3	98.2	12.52	0.85	8.68	2.55	1.69	46.90
YardWaste	4	6.90	14.2	26.3	120.0	45.3	5.30	1.28	650.3	95.9	12.82	0.75	8.49	2.47	1.48	53.49
PecanSh	1	7.10	5.3	9.56	32.6	19.8	4.31	1.14	41.8	54.6	12.24	0.82	6.53	3.67	1.41	44.07
PecanSh	2	7.10	7.35	15.0	50.7	25.2	4.40	1.19	110.2	73.3	13.7	0.90	7.19	3.35	1.44	39.47
PecanSh	3	7.00	8.21	16.4	54.3	31.0	5.21	1.25	149.6	71.0	12.67	0.93	6.52	3.51	1.77	41.83
PecanSh	4	6.90	9.03	20.8	70.4	37.6	5.57	1.22	250.0	80.2	12.09	1.14	7.61	3.87	1.73	42.29

Table A.6, continued.

BiocharTrt	Block	pH	EC	Mg	Ca	Na	SAR	OM	Nitrate-N	K	P	Zn	Mn	Fe	Cu	% Saturation
			dS/m	mg/kg				g/kg	mg/kg							
CotTrash	1	7.10	9.82	25.5	70.1	36.6	5.29	1.95	1.69	257.0	27.82	1.07	8.65	2.80	1.22	47.04
CotTrash	2	7.10	9.55	24.5	67.6	34.4	5.07	1.59	0.52	249.0	28.57	1.06	8.45	2.63	1.79	45.08
CotTrash	3	7.00	8.95	21.4	61.3	35.5	5.52	1.77	1.34	266.0	28.57	1.02	8.55	2.97	1.72	44.08
CotTrash	4	7.10	8.15	20.4	59.0	34.4	5.46	2.24	0.42	234.0	28.38	1.13	9.40	2.97	2.15	44.24
PecanTree	1	6.90	14.9	31.0	125.0	56.8	6.43	1.20	661.4	107.0	12.09	1.04	6.49	2.61	1.67	39.06
PecanTree	2	6.80	18.1	48.4	174.0	77.5	7.35	1.32	930.4	126.0	11.66	1.30	8.35	2.10	2.28	40.03
PecanTree	3	6.80	17.20	36.2	146.0	67.2	7.04	1.17	995.8	122.0	12.09	1.14	7.19	2.22	1.86	40.62
PecanTree	4	7.02	11.8	25.4	87.9	50.1	6.66	1.26	450.1	98.1	12.52	1.29	8.06	2.91	2.41	43.56